ENERGY USE ANALYSIS & TECHNOLOGY FOR ELECTRIC TRANSIT BUSES

By

Pierre R. Hinse

A Thesis Submitted in Partial Fulfillment

of the Requirements for the Degree of

Masters of Applied Science

Automotive Engineering

in the

Faculty of Engineering and Applied Science

University of Ontario Institute of Technology

May 2010

CERTIFICATE OF APPROVAL

Submitted by **Pierre Hinse**

In partial fulfillment of the requirements for the degree of

Master of Applied Science in **Automotive Engineering**

Date of Defence: **April 15, 2010**

Thesis title: Electric Vehicle Technology, Vehicle to Grid, and Energy Analysis

The undersigned certify that the student has presented **[his/her]** thesis, that the thesis is acceptable in form and content and that a satisfactory knowledge of the field covered by the thesis was demonstrated by the candidate through an oral examination. They recommend this thesis to the Office of Graduate Studies for acceptance.

Examining Committee

Remon Pop-Iliev
Chair of Examining Committee

Peter Berg
External Examiner

Greg Rohrauer
Research Supervisor

Co-Supervisor

Mikael Eklund
Examining Committee Member

Examining Committee Member

As research supervisor for the above student, I certify that I have read and approved changes required by the final examiners and recommend the thesis for acceptance:

Greg Rohrauer
Research Supervisor

UNIVERSITY OF ONTARIO INSTITUTE OF TECHNOLOGY

ABSTRACT

Energy Use Analysis and Technology for Electric Transit Buses

By: Pierre Hinse

Chairperson of the Supervisory Committee:

Dr. Greg Rohrauer
Faculty of Engineering and Applied Science

Electric vehicles offer a method of transportation where the energy generation process is moved from the on-board engine to the electrical generation system. The Canadian electrical generation mix has a significant portion of low carbon and renewable sources. This low environmental impact source of energy is then transferred to electric vehicles when they are charged from the grid. This thesis analyses the energy flow for such electric vehicles, particularly buses. Battery systems and charger technology, core to the vehicle operations, are examined; looking at energy flow from plug to wheels. Field data collected from on-board recordings and simultaneous Global Positioning System (GPS) signals were used to develop a new predictive model for an electric bus. The mathematical model for the electric bus was then compared with a similar sized diesel engine vehicle model using the Powertrain System Analysis Toolkit (PSAT). The operational energy cost of the electric bus is contrasted with a similarly sized Compression Ignition (CI) engine bus and was found to be very favourable. Also cost effective battery system upgrades to the present system were analysed for improved return on investment.

Keywords: Transportation, Energy, Battery, Simulation, Green House Gas, Public Transit, Electric Vehicle

ACKNOWLEDGMENTS

The author wishes to express sincere appreciation to Dr. Rohrauer for his research guidance and assistance in the preparation of this paper. In addition, special thanks to Dr. Lemonde for her unwavering financial and emotional support. This work would also not have been possible without the contribution of Mr. Michael Angemeer, President and CEO of Veridian Connections, for the industrial contribution to a National Science and Engineering Research Council study grant, and Ontario Power Generation for equipment sponsorship.

Finally the author wishes to gratefully thank his immediate and extended family.

TABLE OF CONTENTS

LIST OF FIGURES

LIST OF TABLES

Number *Page*

GLOSSARY

A: Ampere

AC_D: Aerodynamic Drag Coefficient Product

AGM: Absorbed Glass Mat, a variation of the PbA battery

APS: Advanced Powertrain Systems, OEM bus manufacturer (closed)

BMS: Battery Management System, the ESS management and control system

CAN: Controller Area Network, communication network layer for automation and control

CARB: California Air Resources Board

CI: Compression Ignition engine

DART: Data Acquisition and Reporting Toolkit, the bus energy logging front end

DOD: Depth of Discharge, estimate of total energy fraction used from a battery

ESS: Energy Storage System, a complete vehicle battery system

EV: Electric Vehicle

F_A: Aerodynamic Drag Force

F_R: Rolling Resistance Force

F_T: Tractive Force

FC: Fuel Cell

g: gravitational acceleration

GHG: Green House Gases

GPS: Global Positioning System

GUI: Graphic User Interface

GVWR: Gross Vehicle Weight Rating

HVAC: Heating Ventilating and Air Conditioning

kWh: kilo-Watt hour

Li: Lithium (chemical element)

LiFePO: Lithium Iron Phosphate, a form of lithium based battery

MWhr: Mega Watt Hour

NEMA: National Electrical Manufacturers Association

NiCad: is a registered trademark of SAFT Corporation, used for NiCd

NiCd: Nickel Cadmium secondary battery

NMEA: National Marine Electronics Association

OEM: Original Equipment Manufacturer

OPG: Ontario Power Generation

Pb: Lead (chemical element)

PbA: Lead Acid secondary battery

Primary Cell: Single use electrochemical cell

RTD: Resistive Temperature Device

Secondary Cell: Rechargeable electrochemical cell

SOC: State of Charge

SOH: State of Health

T/C: Thermocouple

UOIT: University of Ontario Institute of Technology

V: Volt

VRLA: Valve Regulated Lead Acid, a variation of the PbA battery

W: Watt

ZEV: Zero Emission Vehicles

ϱ: rho, density of air at standard conditions

Ω: ohm, electrical resistance

Chapter 1

INTRODUCTION

Electric vehicles offer a method of transportation where the energy generation process is moved from the on board engine to the electrical generation system. The Canadian electrical generation mix is mostly comprised of low-carbon generating or renewable sources, and this low environmental impact energy is then transferred to electric vehicles when they are charged from the grid. The present work analyses the energy flow in electric vehicles. The focus is on the energy flow and efficiency from the plug to the wheels in the case of an electric bus. The Canadian electrical generation mix is different from province to province and ranges in CO_2 equivalent (eq.) generated from electricity production between 1.8 g CO_2 eq. /kWhr for Quebec to 774.1 g CO_2 eq. /kWhr for Nova Scotia. The national average per kWhr is 189.3 g CO_2 eq. /kWhr [Canadian Federal Government]. This research continues previous work carried out by Santa Barbara Electric Transportation Institute (SBETI) in California. The longitudinal SBETI research performed over the course of 8 years focused on: driver energy management, vehicle performance and applicability, battery life, charger performance, maintenance and operational costs, and air quality benefits [Griffith, Gleason].

Chapter 2 describes selected battery technologies, the heart of an electric vehicle. Differences between battery chemistry, energy and power properties for a variety of cell types are considered. Life expectancy is also examined as well as replacement costs.

Chapter 3 deals with Battery Management Systems (BMS); these play an important role in the protection and control of the energy storage system. The various functions of a BMS are identified and described.

Chapter 4 describes the experimental electric buses used to perform this research, including specifications and steps taken to recondition and license the vehicles.

Chapter 5 comments on the electric buses field tests and shows how these were used to build a computer model of the buses. Compared to a model of a similar sized diesel bus, the cost of operation of both in terms of energy is compared.

Chapter 6 examines the case for Lithium Ion energy storage upgrades from an economic viewpoint.

Chapter 7 concludes and indentifies the contributions the author made in the course of this work and proposes future directions for research.

Chapter 2

ENERGY STORAGE SYSTEM

Summary

The heart of an Electric Vehicle (EV) is its battery system. In this chapter, different battery technologies are examined, such as: Flooded Lead Acid (PbA); Valve Regulated Lead Acid (VRLA); Nickel Cadmium (NiCd); Nickel Metal Hydride (NiMH) also known as Nickel-Hydrogen; Lithium-ion Cobalt (Li); and Lithium Iron Phosphate (LFP). Initial cost and cost per unit energy for those batteries most appropriate in electric vehicles are identified. Differences result from cell chemistries in relation to their technological capabilities and limitations balanced against cost.

Introduction

Self propelled vehicles require energy storage; this can take the form of chemical, mechanical, or electrical energy. Electric vehicles require electrical energy storage. Of all the systems on board an electric vehicle, the Energy Storage System (ESS) is the most critical to its operation. The ESS occupies a significant proportion of the mass and the volume of a vehicle. As a result, this chapter focuses on the most critical component of the ESS: Secondary Batteries [Raman, et al., 2004].

Three main battery chemistry types are considered: Lead Acid (PbA), Nickel Cadmium (NiCd), and Lithium-ion (Li). Each type can be separated into different chemical and mechanical property sub-groups. Briefly explored and studied are their respective qualities such as: chemistry, energy density, power density, and system complexity. Also considered are their respective sensitivity to: temperature, mechanical abuse, and maintenance requirements. Finally, the initial cost, and the life expectancy effect on costs are examined.

Common Terms

When discussing battery systems several common terms are used to describe characteristics of the batteries:

- C Rate: a quantity that describes the capacity of a cell to charge or discharge in terms of its columbic capacity. Example: a 1 Ah ½C discharge rated cell can provide 0.5 A for two hours.
- SOC: State of Charge, a percentage of the charge status of the cell from 0% to 100%.
- SOD: State of Discharge, 1 – SOC (%)
- SOH: State of Health, often cells will degrade, when this occurs the full rated capacity is unavailable, the proportion remaining is described in terms of a percentage of its initial capacity.

Temperature Effects

All batteries have a temperature range that favours their performance or extends their life span; these ranges are not necessarily overlapping. Some batteries will favour operation at higher temperatures. For example, lead acid (PbA) batteries offer highest performance at 40°C. Conversely a colder environment may cause electrolyte freezing effectively halting chemical processes in the cells or physically damaging the container. Batteries are chemical devices, reactions become "sluggish" as the temperature drops from the optimal range. As a consequence of colder environments the battery output will be decreased, this effect is not permanent and the capacity is restored as the temperature rises.

Hot environments may cause deterioration of battery cells, oxidation of the electrodes or the vaporization of the electrolytes. Some cells may suffer electrolyte deterioration as the chemicals decompose. The process of charging and discharging batteries generates heat; the heat can adversely affect the cells if not managed properly.

Metals present in batteries such as copper will exhibit a positive temperature coefficient. The internal resistance will increase as the temperature increases; conversely chemical processes exhibit a decreasing resistance. (This is true to a maximum temperature where the electrolyte decomposition overcomes the chemical reaction speed advantages.) [Fuhs]

Lithium cells will exhibit a longer life span when stored at temperatures just above 0°C, but will perform to their full capacity anywhere from 0°C to 40°C [Wenige et al.].

Lead Acid Batteries

Lead Acid cells consist of two subtypes, Flooded Lead Acid (PbA), and Valve Regulated Lead Acid (VRLA). Each can be mechanically arranged for different characteristics of either high momentary current discharge "Starting Batteries" or deep cycling for large Depth of Discharge (DOD). The chemistry in all four is essentially similar; two plates, one consisting of metallic lead (Pb) and the other of lead sulphate ($PbSO_4$) are immersed in an aqueous solution of sulphuric acid (H_2SO_4) [Buchmann, 2001]. A voltage potential is generated by the separation of the plates and the affinity of the lead ions to combine with the sulphate ions. Discharge current is generated when electrons are liberated during the recombination of the ions. During charging, lead and sulphate ions are forced apart by the applied voltage on the plates, and the metallic lead is re-deposited on the plate. As shown in Equation 1, sulphate ions balance the hydronium (H_3O^+) ions (Figure 2) [Weisstein, 1996].

$$PbSO_4(s) + 5H_2O(l) \overset{Cathode}{\longleftrightarrow} PbO_2(s) + 3H_3O^+(aq) + HSO_4^-(aq) + 2\acute{e}$$

$\epsilon^0 = 1.685eV$ "Gibbs Energy" under standard conditions (298°K, 1 molar)

$$PbSO_4(s) + H_3O^+(aq) + 2\acute{e} \overset{Anode}{\longleftrightarrow} Pb(s) + HSO_4^-(aq) + H_2O(l)$$

$$\epsilon^0 = -0.356eV$$

Equation 1, Lead Acid Cell: Charging

The Flooded Lead Acid (PbA) cell has a charge/discharge curve as illustrated in Figure 1, the relationship between SOC and the voltage at the terminals is not linear. Although, the specific gravity does follow a linear relationship with the SOC. Specific gravity is a complex parameter to monitor during use, most systems use a coulomb counting technique with a correction method at the end of the charge/discharge cycles. The charge cycle exhibits a termination voltage once the cell has reached 100% SOC, current can continue charging the cell at this point at the expense of electrolyte.

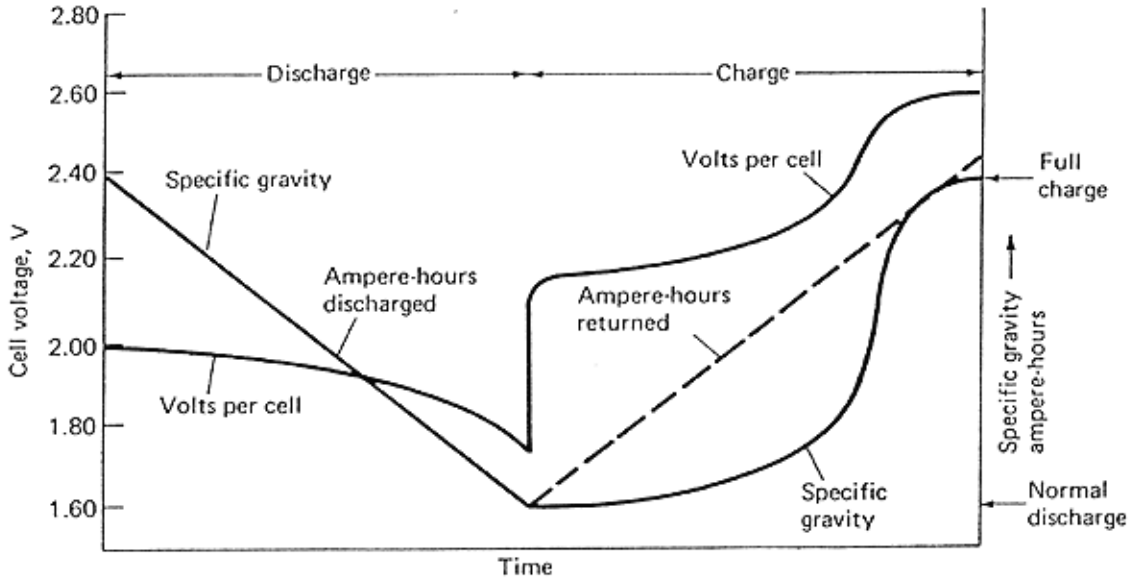

Figure 1, Lead Acid Cell: Voltage/Gravimetric/Capacity plot
(from [Typical Voltage and Specific Gravity Characteristics of a Lead-acid Cell])

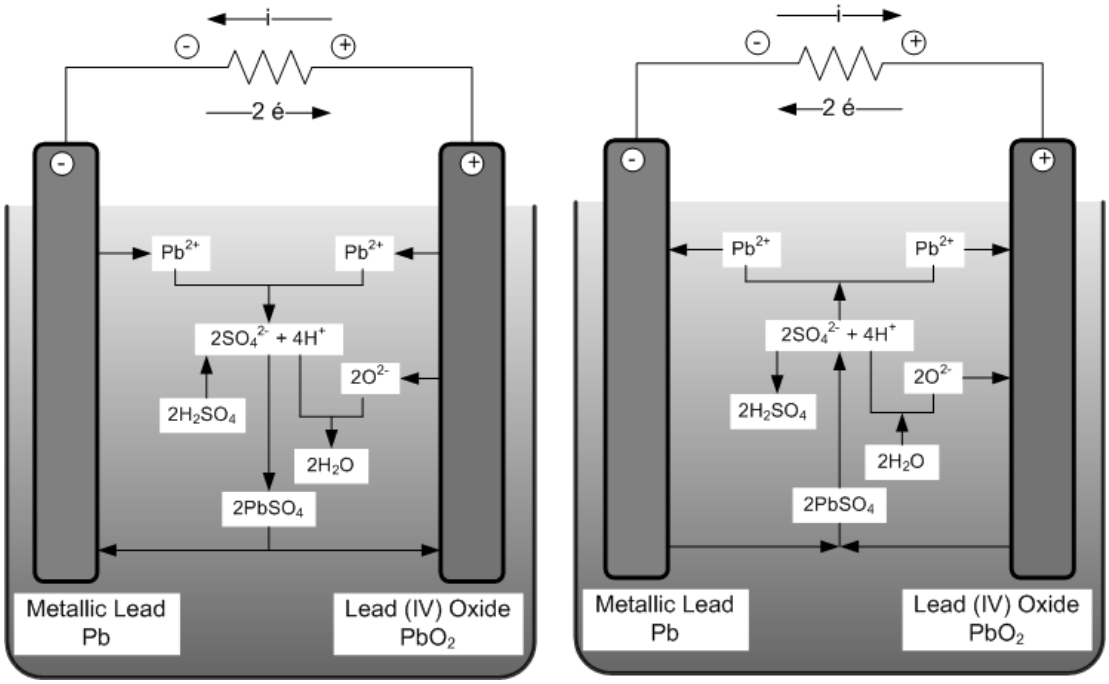

Figure 2, Lead Acid Cell: Discharging (left), Charging (right)

VRLA can be separated into two subgroups: Absorbent Glass Mat (AGM) and Gel. Often called *sealed lead acid* they are constructed with a "recombinant" system to form water from the emitted Hydrogen and Oxygen generated at the plates. This water replaces the electrolyte lost

during the electrolysis of the water. The AGM battery also includes a safety valve to release pressure in the event that gasses are formed faster than the recombinant mechanism can absorb them. This design results in higher energy density since less electrolyte mass is required to "flood" the battery [Buchmann, 2001]. Several disadvantages are encountered while using VRLA batteries: comparatively low energy and power density reduces the available range, performance, and load capacity of the vehicle. The lower cyclic life capacity of the cells compared to the NiCd or Lithium cells described below imply significant maintenance and replacement requirements, in return nullifying a proportion of the savings from not using fossil fuels. Typical replacement periods are 3 years / 400 – 600 cycles [Buchmann, 2001].

Nickel Batteries

Nickel based cells are comprised of two main types: Nickel Cadmium (NiCd) with a Potassium Hydroxide electrolyte, and Nickel Metal Hydride (also known as Nickel-Hydrogen) [Buchmann, 2001].

Flooded Nickel Cadmium cells use a Cadmium plated negative electrode, and a nickel Hydroxide ($NiOH_2$) plated (+) electrode with a fibre separator between the plates. The electrolyte consists of a 30% Potassium Hydroxide solution. As the cell is discharged, the Cadmium moves into the solution and combines with 2 hydroxide ions while releasing 2 electrons. At the Nickel hydroxide positive electrode, Nickel oxide (NiO2) combines with 2 water molecules and deposits Nickel hydroxide ($Ni(OH)_2$) on the electrode, while releasing 2 hydroxide ions and absorbing 2 electrons. As indicated in Equation 2 (Figure 3) [Buchmann, 2001].

$$Ni(OH)_2(aq) + 2OH^-(aq) \overset{Cathode}{\longleftrightarrow} NiO_2 + 2H_2O(l) + 2\acute{e} \quad \epsilon^0 = -0.8277eV$$

$$Cd(OH)_2(aq) + 2\acute{e} \overset{Anode}{\longleftrightarrow} Cd(s) + 2OH^-(aq) \quad \epsilon^0 = -0.40eV$$

Equation 2, NiCd Cell

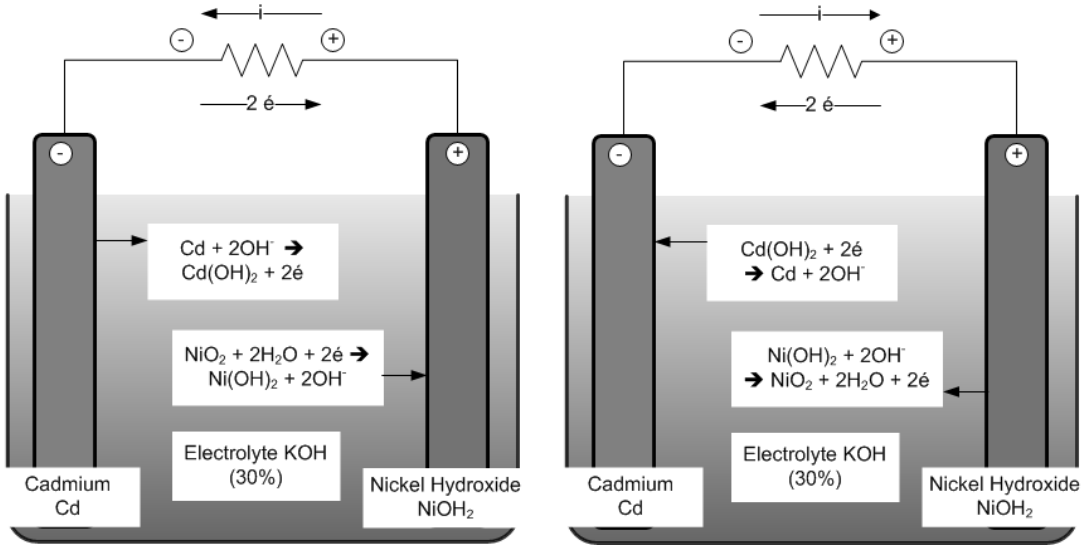

Figure 3, NiCd cell, Discharging on left and Charging on right

The NiCd cells exhibit good cyclic life. For example, as demonstrated in this research NiCd cells still had an average 55% capacity remaining after 12 years, despite lack of care while in use and storage. A 20 year lifespan consisting of 2000 charges-discharge cycles is supposedly possible with care. Although the power and energy densities are higher than PbA batteries, a large traction battery system for a vehicle such as a small transit bus still has a mass of 2500kg for 100kWh [Rohrauer, 2009 A].

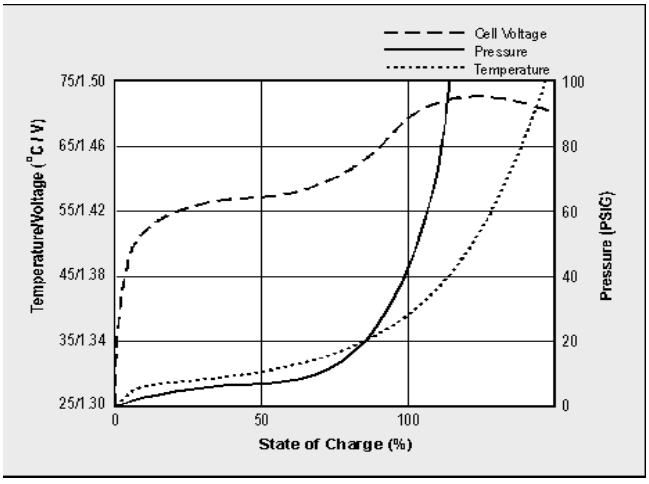

Figure 4, NiCd cell, Temperature/Pressure/Voltage Profile
(from [Buchmann])

Figure 4 shows the result of charging a NiCd or NiMH cell, charge termination should occur on the negative voltage slope immediately after reaching 100% SOC. If charging is continued electrolyte loss is incurred.

Nickel Metal Hydride (NiMH) cells are quite popular as traction batteries for hybrids currently in use by Ford, General Motors, Honda, Toyota, and others [Idaho National Laboratory, 2006]. In Figure 5, NiMH cells have an anode (-) in a metal alloy capable of absorbing and releasing hydrogen, the cathode (+) is composed of nickel hydroxide, immersed in an electrolyte composed of potassium hydroxide, sodium hydroxide, and lithium hydroxide. NiMH cells have a nominal voltage of 1.2V. In smaller formats; the cells are sealed with a pressure release device at one end. In the larger formats (>60 Ah), the cells are typically open. NiMH cells require a precise charge level monitoring to control gaseous formation and venting. Charge monitoring helps prevent electrolyte loss and extends the useable life of the cells. Thermal run-away through overcharge is a real concern however, so charge termination at the appropriate point is critical. NiMH cells have good energy density and in controlled conditions have sufficient lifespan for transportation use [Buchmann, 2001].

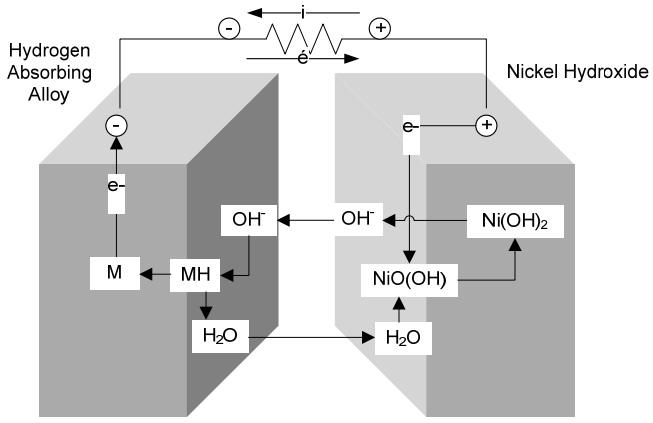

Figure 5, NiMH Cell, Discharging

Lithium Ion Batteries

Lithium Ion batteries have a large number of types and chemistries [Buchmann, 2001]; this study concentrates on a few types that were available for our research. One cell of interest was the Sony 18650, a 3.7 Volt 2.2 Ah Cobalt Hard Carbon anode based cylindrical cell. The cell

consists of a cobalt oxide positive electrode and graphite carbon negative electrode. The cells exhibit the following energy properties (Table 1):

Table 1, Sony Cell Characteristics
(from [Sony, 2001])

Power Density	121 W/kg
Energy Density	121 Whr/kg
Volumetric Energy Density	3.67 kWhr/L
Cyclic Life	> 500 Cycles

These cells cannot repeatedly sustain charge/discharge currents of more than 1C (page 3) without severely shortening lifetime nor a DOD of greater than 80% (Figure 6) [Sony, 2001]. Product recalls have been issued in the past for thermal events caused by lithium cells in portable computers [Vallese, and Wolfson, 2006].

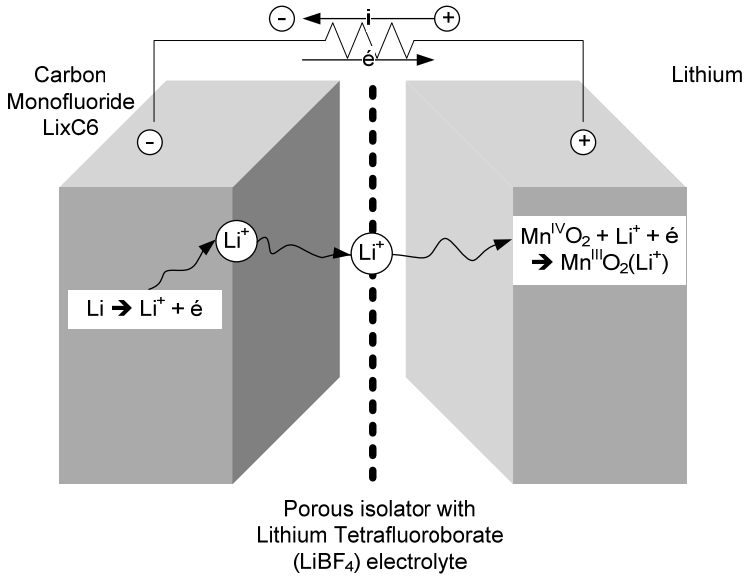

Figure 6, Li $(CF)_n$ Lithium polycarbon monofluoride cell, discharging

For the case of Lithium Iron Phosphate chemistry, the A123 "M1" cell, a 3.2 Volt 2.3 Ah Iron Phosphate based cell, is exemplary. In this cell, nano-phosphate materials are added to the lithium cathode, hence it can safely sustain charge/discharge rates of 35C, with DOD approaching 0% [Codecà, et al., 2008].

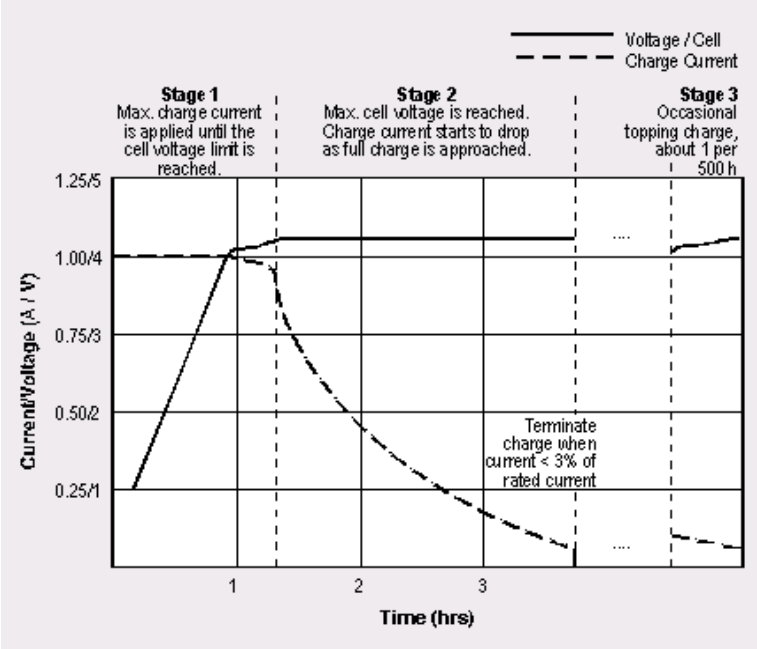

Figure 7, Lithium cell, Charging Profile
(from [Buchmann])

Figure 7 show the charging profile of a lithium cell, during the constant current phase the voltage rises rapidly to a voltage plateau. The voltage is maintained at this level until the current decreases to approximately 3% of the C rate. It is important to stop the charge sequence at this point to prevent the overcharging the cell, increasing the risk of failure.

Table 2, Common Battery Metal Properties
(From [Weast, 1975])

Metal	Name	Mass (g/mol)	Gibbs Energy (eV)	Density (g/cm3)	Electro-chemical Equivalence (Ah/g)	Number of electrons	Mass per electron	Energy Density eV◦é/g
Li	Lithium	6.94	-3.045	0.53	3.86	1	6.94	0.44
Al	Aluminum	26.9	-1.706	2.70	2.98	2	13.4	0.13
Mg	Magnesium	24.3	-2.375	1.74	2.20	2	12.2	0.20
Na	Sodium	23.0	-2.7109	0.97	1.16	1	23.0	0.12
Fe	Iron	55.8	-0.445	7.85	0.96	2	27.9	0.016
Ni	Nickel	58.7	-0.23	8.90	0.91	2	29.4	0.008
Zn	Zinc	65.4	-0.7628	7.10	0.82	2	32.7	0.023
Cd	Cadmium	112	-0.4026	8.65	0.48	2	56	0.007
Pb	Lead	207	-0.1205	11.3	0.26	2	103.5	0.001

Lithium polymer cells are comprised of a thin Lithium oxide anode and a conductive cathode deposited on an aluminum substrate with a carbon/graphite coating. Lithium polymer cells currently have the best energy density of the commercially available secondary cells. In Table 2, several common battery metals are listed with their properties; the metals are ordered by increasing molar mass. To create the last column: Energy Density, the number of electrons commonly participating in electrochemical cells per atom, is divided into the molar mass and multiplied by the standard potential. This metric represents the theoretical energy obtained if all the metal present participated in the reaction. This metric is incomplete and can only be used for an indication of the potential energy stored in a cell; nevertheless it shows lithium has an advantage compared to the other entries [Buchmann, 2001]. The challenge is to design an electro-chemical cell that will realise the full energy potential of lithium.

Battery Selection

The selection of one appropriate battery for use in an electric vehicle is dependent on several factors: initial cost, size, voltage, current, power, energy, temperature range, heat generation, availability, maintenance, safety system requirements, and life cycle costs. Considering only power and energy densities, Figure 8 shows different cell chemistries in relation to their technological capabilities [Axsen, et al., 2008]. In Figure 8, five additional cell points were added for: A123 M1; Kokam Power; Electrovaya MN; Kokam Energy; and LG Chem E1.

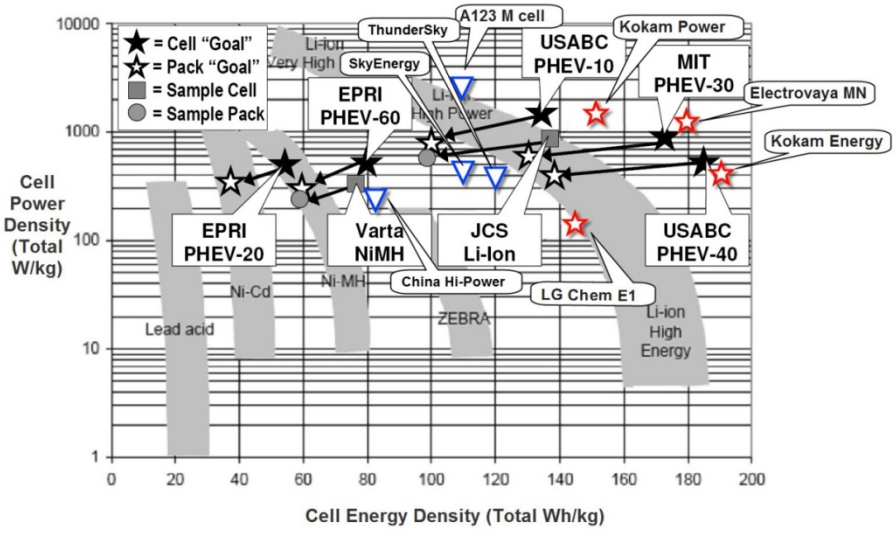

Figure 8, Ragone Plot for Battery Chemistries

(from [Axsen, et al, 2008])

A study of Figure 8 shows that the most interesting cells are the Electrovaya MN and Kokam Energy because of their high cell energy density and adequate power density. However when choosing battery options, other considerations must also be taken into account. One must consider the issues of costs and availability.

Costs and Availability

Several Ford Ranger EVs were available in our laboratory, with their ESSs in varying states of health. A valuable exercise was to consider available secondary cells for replacement into a Rangers' ESS. The simplest replacement would have been to use the same VRLA modules as specified by Ford (i.e.: BXE-202), but these are no longer available. A close equivalent was found to be the Panasonic EC-FV0890; however the distributor requires an order of at least a million units to recommence production [HIRO Energy]. This was unfortunate and not found to be a practical solution. Extensive consideration of other lead acid battery suppliers led to the construction of Table 3.

In each case, the number of modules required was based on system voltage and energy storage requirements. Most were either found to be too large or too heavy for the dimensions of the ESS case, except for a few options.

A full evaluation must also consider the initial purchase cost and the life cycle usage of the cells. The expected power delivery of the cells over their estimated cycle counts was calculated. Most exceeded the original BXE-202's expected power delivery. If the initial purchase price is factored into the consideration, then cost per MWh for the life of the cells can be estimated. Ignoring the models that were too large or heavy, the only lead acid candidates remaining were found to be: CSB XTV12750; Odyssey PC1250; and Powersafe 12VE45-VE, at respectively ≈$1225/MWh; ≈$2500/MWh and ≈$791/MWh

Alternative cell technologies were also considered, namely lithium and NiMH. However, this change in technology would have required a Battery Management System (BMS), adding to the cost. Even so, of the lithium and NiMH solutions, the HP-50160282 manufactured by China HiPower would be the lowest cost per MWh at $115/MWh [Zhao, 2010]. Clearly, for practical purposes, the Ford Ranger ESS can be rebuilt with VRLA technology. However, it is equally clear that a lithium based ESS is a superior choice but requiring a higher capital outlay.

Table 3, Battery technical data for purposes of battery replacement analysis
(from various industrial sources, compiled by author)

	Brand	BCI Group Size	Model	V	Parallel #	series #	Quant	Cycles	%DOD	Ah/cell	Ah/module	L	W	H	Mass/cell	$/cell	$ for 312V	kWh	Lifetime MWh	mass sum (kg)	mass sum (lb)	volume (L)	Packing Factor x 1.3	kWh/L	kWh/kg	$/Lifetime MWh	$/kWh pack	$/kg	Comment
Lead - Acid	Ford		BXE-202	8	1	39	39	300	50	70	70	387	114	168	23			11	3.3	909	2000	291	378	1.93	0.62				original, not in production
	Panasonic		EC-FV0890	8	1	39	39	400	50	90	90	388	116	175	22			14	5.6	858	1888	307	399	2.34	0.84				unavailable
	US Batt		US-8VGC	8	1	39	39	200	50	165	165	260	181	276	29.5	53	2067	26	5.1	1152	2535	508	660	2.60	1.15	402	80.30	1.79	Will not fit, too heavy
	Trojan	GC2	T-890	8	1	39	39	200	50	165	165	264	181	276	31.4	122	4758	26	5.1	1223	2691	514	669	2.57	1.08	924	184.85	3.89	Will not fit, too heavy
	Odyssey	31	PC2150	12	1	26	26	200	50	100	100	330	173	239	34.1	300	7800	16	3.1	886	1950	354	461	3.39	1.35	2500	500.00	8.80	Tight fit
	US Batt	8V	11-4-1	8	1	39	39	200	50	142	142	489	191	273	28	228	8892	22	4.4	1092	2402	992	1289	1.15	1.04	2007	401.41	8.14	Will not fit, too heavy
	Trojan	GC8	T-875	8	1	39	39	200	50	170	170	264	181	276	29	282	10998	27	5.3	1131	2488	514	669	2.64	1.20	2074	414.71	9.72	Will not fit, too heavy
	US Batt	8V	13-4-2	8	1	39	39	200	50	155	155	546	191	273	28	292	11388	24	4.8	1092	2402	1108	1440	1.12	1.14	2355	470.97	10.43	Will not fit, too heavy
	US Batt	8V	17-4-3	8	1	39	39	200	50	215	215	699	191	273	35	380	14820	34	6.7	1365	3003	1417	1842	1.21	1.26	2209	441.86	10.86	Will not fit, too heavy
	US Batt	8V	19-4-4	8	1	39	39	200	50	240	240	679	216	283	50	407	15873	37	7.5	1950	4290	1617	2102	1.19	0.98	2120	423.96	8.14	Will not fit, too heavy
	CSB		XTV121000	12	1	26	26	400	50	100	100	343	170	278	46	300	7800	16	6.2	1188	2614	421	548	2.85	1.01	1250	500.00	6.56	Will not fit, too heavy
	CSB		XTV12850	12	1	26	26	400	50	85	85	343	170	218	33	250	6500	13	5.3	868	1910	331	430	3.09	1.17	1225	490.20	7.49	Tight fit
	CSB		XTV12750	12	1	26	26	400	50	75	75	261	169	214	30	215	5590	12	4.7	772	1699	245	319	3.67	1.17	1194	477.78	7.24	Potential Solution
	UPG	31	UB121100	12	1	26	26	400	50	110	110	328	172	254	33	190	4940	17	6.9	863	1898	372	484	3.54	1.53	720	287.88	5.73	Will not fit
	Exide	981	8V-MD	8	1	39	39	400	50	146	146	486	191	273	25	150	5850	23	9.1	975	2145	985	1281	1.18	1.20	643	257.14	6.00	Will not fit, too heavy
	Exide	1	"8-1"	8	1	39	39	400	50	46	46	230	175	229	25	105	4095	7	2.9	975	2145	358	466	1.02	0.38	1432	572.73	4.20	Will not fit, too heavy
	Exide	GC2	GC8V-110 8V	8	1	39	39	400	50	103	103	262	181	291	31	105	4095	16	6.4	1212	2666	537	698	1.53	0.68	639	255.68	3.38	Will not fit, too heavy
	Powersafe		12VE45-VE	12	2	26	52	300	50	45	90	226	139	206	20	64	3332	14	4.2	1014	2231	337	437	3.21	1.07	791	237.33	3.29	Will not fit, too heavy
	DEKKA	31	8G27M	12	1	26	26	500	50	75	75	329	171	238	32	200	5200	12	5.9	824	1813	348	453	2.59	1.09	889	444.44	6.31	Will not fit
Lithium	Edan		IFP337194s1200e	3.2	9	98	882	300	70	12	108	96	71	33	0.4	15	13230	24	7.1	353	776	198	258	1.74	0.98	1860	558.04	37.50	
	Thunder Sky		LFP90AHA	3.7	1	85	85	2000	70	90	90	145	220	68	3	145	12325	20	39.6	255	561	184	240	1.81	1.31	311	622.05	48.33	
	Thunder Sky		LCP100AHA	4.0	1	78	78	2000	70	100	100	145	220	61	3	160	12480	22	43.7	234	515	152	197	2.64	1.71	286	571.43	53.33	
	Kokam		SLPB90216260	3.7	3	85	255	2500	80	40	120	9	215	220	0.9	250	63750	30	75.5	230	505	109	141	4.09	1.93	845	2111.49	277.78	
	SONY		US26650	3.6	36	87	3132	1000	70	2.8	101	27	27	66	0.08	20	62640	22	22.1	260	572	146	189	2.49	1.40	2834	2834.47	240.96	
	K2 Energy		LFP26	3.2	32	98	3136	1000	70	3.2	102	26	26	65	0.08	12	36064	22	22.5	257	566	140	182	2.33	1.27	1604	1604.35	140.24	
	K2 Energy		LFP200ES	12.8	7	25	175	1000	70	16	112	140	104	69	1.73	249	43575	25	25.1	302	665	175	227	8.21	4.74	1737	1736.89	144.16	
	A123		M1	3.3	44	95	4180	5000	80	2.3	101	67	26	26	0.07	21	87780	25	126.9	293	644	188	244	1.78	1.14	692	3458.50	300.00	
	Hi-Power		HP-50160282	3.2	1	98	98	3000	70	100	100	282	160	50	4	110	10780	22	65.9	343	755	221	287	1.45	0.93	164	491.07	31.43	
	A123 clone		ANR26650M1A	3.3	36	100	3600	3000	70	2.3	83	67	26	26	0.07	5.6	20160	19	57.4	252	554	163	212	1.68	1.08	351	1054.02	80.00	
Ni MH	Nilar		24V 9Ah NiMH	24.0	10	13	130	2000	70	9	90	279	129	55	3.9	233	30333	20	39.3	507	1115	257	335	8.39	4.26	772	1543.21	59.83	

Conclusion

Several ESS cell technologies are readily available for EV use. The lower initial cost lead technologies are an attractive option, but their short life expectancy (due to their lower endurance of charge-discharge cycles) makes them more expensive over the life of the vehicle than the newer lithium based cells. Lithium cells require a greater initial outlay, and also need additional cell monitoring infrastructure compared to lead based cells. However, lithium cells have much higher expected cycle counts, and also provide significantly increased energy density thus making the vehicle lighter. A lighter ESS decreases the energy consumption per kilometre providing longer range with the same energy capacity ESS.

A discussion on batteries cannot made without consideration of the W. Peukert empirical equation, Wilhelm Peukert developed the equation from detailed observations of lead acid batteries in 1897 [Peukert].

$$C_{n1} = C_n \left(\frac{I_n}{I_{n1}}\right)^{pc-1}$$

Equation 3, Derived Peukert Equation
(from [Doerffel, Sharkh])

Where: C_{n1} is the capacity at a higher discharge rate, C_n is the nominal capacity, I_n is nominal discharge current, I_{n1} is the higher discharge current, and *pc* the Peukert constant for the particular cell. For lead acid batteries the *pc* was found to be about from 1.1 to 1.47, for lithium batteries the temperature has a greater effect on remaining capacity than the Peukert effect, where the *pc* is approximately 1.0 [Doerffel, Sharkh][Wang et al.].

When lead acid batteries are discharged at usual rates (typically greater than 0.1 C), the Amp Hours (AH) supplied by the battery will less than its rated capacity based on C/20. Other chemistry batteries will have a similar characteristic, but for each the *pc* will be different. This characteristic will also vary across batteries of the same chemistry, but of different manufacturing batches.

"The loss of capacity at a high discharge rates can be explained to be due to a decrease in the number of active centers in the positive active material and a rapid increase in the resistance of the interface between the grid and the lead dioxide active material" [Doerffel, Sharkh].

The observed loss is not permanent, as the remaining capacity of the cells is restored after a rest period. Continued discharge can be achieved to reach a state where the cell is completely discharged. In lithium based cells it has been noted that the temperature rise caused by the rapid discharge (the increased temperature accelerates the chemical reaction, and the dispersion of ions) had a greater effect on the cell capacity then the Peukert effect [Doerffel, Sharkh].

In the next chapter, the use of a battery management system to monitor and control the status of the individual modules in an ESS is considered.

Chapter 3

BATTERY MANAGEMENT SYSTEMS

Summary

Large batteries require a management system to monitor the state of individual cells, and provide communications and control. In this chapter, battery management systems are described and their need is explained. More sophisticated systems are shown to include thermal management and cell level balancing to maximise power output and throughput.

Introduction

Few large battery systems can be left unmonitored; in large arrays, a single cell or module can be at risk of catastrophic failure or become defective, going unnoticed from the overall voltage/current characteristics of the aggregate system. For example, a 360 V, 54 module NiCd ESS consisting of 6 V modules can have a completely defective module and yet only shows a 6 V difference for the system. Considering that the potential typically drops 50 Volts under load, this will go unnoticed to the vehicle operator. A Battery Management System (BMS) then becomes a critical component for monitoring the health of a large ESS [Woodbank Communications Ltd, 2005].

Figure 9 illustrates a complete vehicle energy management diagram, showing the possible functions implemented within a BMS. In order to accomplish this, a BMS requires sensors for temperatures and voltages. BMS functions include State of Charge (SOC), State of Health (SOH), alarm functions, diagnostics, data logging, and control. Communications to the vehicle and a Graphical User Interface (GUI) are valuable additions to any BMS. ESSs are enhanced by providing a range of charge-discharge operations unavailable without close monitoring of the individual cells.

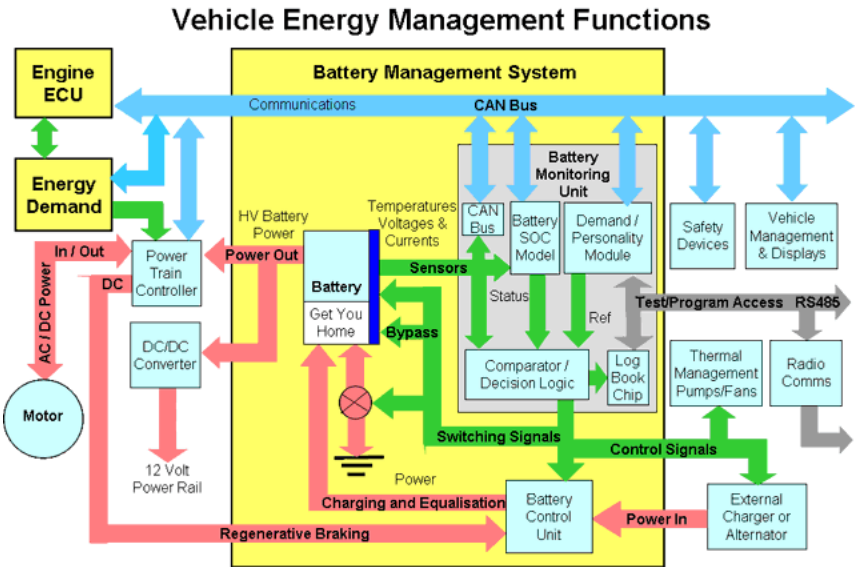

Figure 9, Vehicle Energy Management Functions
(from [Woodbank, 2005])

BMS Technology

Based on a study of available BMS's, Table 4 was constructed, grouping BMS functions into categories by order of complexity and function. The goal of Table 4 is to categorize different BMS functions in ascending order of cost/complexity. The simplest is the Voltage/Current/Power combination; this type only monitors the ESS output characteristics. Although a significant indication of ESS health can be inferred from the energy used in relation to the Voltage, as mentioned previously, a single cell or module can fail catastrophically without significant indication.

As can be seen from Table 4, a wide range of solutions may be implemented where cost and complexity are significant overriding factors in the design. A BMS in its most simple incarnation would provide battery pack voltage indication.

The Data Acquisition and Reporting Toolkit (DART) Energy monitor found on the UOIT shuttle buses is a slightly more complex design with voltage, current, power, and speed logging [SBETI, 1997][Rohrauer, 2009 A]. Original Equipment Manufacturer (OEM) vehicles such as the GM S10 EV have a monitoring and control system that implements module level voltage monitoring along with a thermal management system running from the vehicle's heat pump,

simultaneously providing the operator with voltage, distance to empty, current indications, and a HVAC system [Ritchie, Howard, 2006].

Table 4, BMS Technology Map

Function	Purpose	Solution		
Voltage	Relative SOC	Resistor Divider	Electronic Amp.	DC/DC Converter
Current	Loading Indication	Shunt	Shunt/isolator	Hall Effect
Power	Loading Indication	Calculation from above		
Energy	Relative SOC	Calculation from above		
Temp.	Relative SOH	RTD	T/C	Infra-red
SOC/DOD	SOC/DOD	Calculation from above		
SOH	SOH	Calculation from above		
Ventilation	Cooling / gas venting	From outside	From habitat	Closed system
Heating	For cold temps.	Resistive from ESS	Resistive from PWR Inlet	Freon
HVAC	Cool/Heat Control	Ventilation	Glycol Loop	Freon
Communications	Indication to operator	Hard wire	serial	CAN
Zone Voltage	Relative SOH	Resistor Divider	Electronic Amp.	DC/DC Converter
Zone Temp.	Area SOH	RTD	T/C	Infra-red
Cell Temp.	Cell SOH	RTD	T/C	Infra-red
Cell Voltage	Cell SOH	Resistor Divider	Electronic Amp.	DC/DC Converter
Cell Balancing	Maximize Useable SOC Range	Bypass/Shunt	Flying L/C	
		➔ ➔ Increasing Cost & Complexity ➔ ➔		

BMS Thermal Management

A critical component of a BMS is thermal management. In its most simple implementation, a shut down can be initiated when temperature reaches a critical point. More sophisticated systems use active management of thermal characteristics by implementing Heating Ventilation and Air Conditioning (HVAC). In consumer electronics the small size and low cell

count result in a small total energy footprint for the ESS; a thermal event can usually be contained safely. In vehicles, the large sizes of the cells multiplied by the number of cells imply a significant concern for safety. Another element that compounds the issue is that the vehicular ESS must also function in environments that can include extremes from arctic cold to desert heat. Low temperature extremes also limit the cell's capacity to supply energy; high temperatures can potentially degrade the electrolyte and limit the expected life.

Lithium batteries have a tendency to ignite when overcharged or overheated [Ritchie, Howard]. In these cases, the metal-oxide cathode is destabilized and releases oxygen, which can then initiate an exothermic reaction between the electrolyte and the metal on the anode. The proximity of the neighbouring cells can lead to a cascading reaction. Cells manufacturers refer to this as "vent with flame" or "thermal runaway" [Beauregard, 2010].

Such thermal issues can be addressed by intrinsic means or passive/active means [Ritchie, Howard]. The chemistry of the cells can be changed to be more durable and less thermally sensitive through combinations of materials such as iron phosphate cathode (LiFePO4) (which has a stable oxidation state) and nano-titanate anode (LiTi12O5) (which does not accumulate lithium metal). For active cooling means, the present use of electrically powered HVAC systems takes energy from the ESS and consequently reduces the vehicle's range [Rohrauer, 2009 B].

Current research is exploring employing passive materials to attenuate the thermal changes during drive cycles, and to delay the onset of the electrically active HVAC system to running only when the EV is recharging. Thus the energy can be supplied by the electrical distribution system instead; thereby effectively offloading the ESS [Rohrauer, 2009 B].

Cell Balancing

All cells are different even when selected from the same part number, measured capacity or manufacturing batch. As cells are charged and discharged over time, these differences manifest themselves as a drifting State of Charge (SOC): as a result cell charge levels will continue to drift over time if no action is taken. A low SOC cell in a series string will effectively shutdown the ESS before all cells have reached that point, preventing the system from using the energy

remaining in the higher SOC cells. This effect is illustrated in Figure 10 where the SOC is plotted over several cycles.

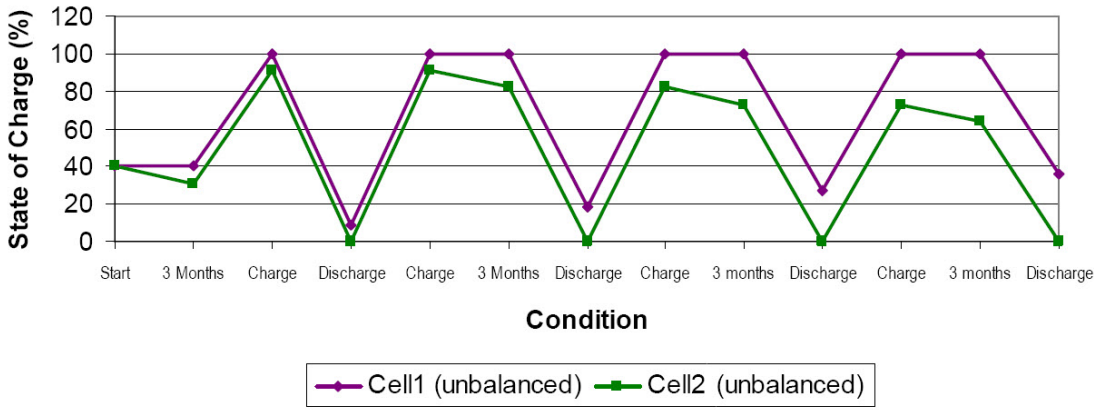

Figure 10, Unbalanced Battery Cell Voltage
(from [Martinez, 2005])

Cell balancing can use three methods for charging the cells at a lower SOC to a level equivalent to the rest of the ESS:

- If the cells allow slight over charge, then continued charging past 100% will allow the lower SOC cells to "catch up". This method is commonly used with lead acid or nickel cadmium for example.
- A zener diode bypass system to shunt part of the charging current around the high SOC cells, allows the low SOC cells to receive a top up charge.
- A charge shunting shuttle mechanism to remove energy form high SOC cells and send this energy to the low SOC cells.

Conclusion

The BMS is a critical component of the ESS for cells that cannot be routinely overcharged. Both PbA and NiCd cells can sustain some overcharge at the expense of electrolyte loss to balance lower SOC cells; this can be accomplished in the charge algorithms. However, NiMH and lithium type cells cannot safely accept current past the 100% SOC level; consequently, the BMS must implement other strategies to protect the ESS.

Chapter 4

APS SHUTTLE BUS

Summary

The previous two chapters have provided an overview of two key systems unique to electric vehicles, the Energy Storage System (ESS) and the Battery Management System (BMS), including some of the challenges facing such systems in a normal operating environment. The present chapter describes the specific electric vehicle whose repair, operation, and modelling is a major focus of this research work.

Introduction

This chapter summarizes the acquisition, rehabilitation, and performance study of two electric buses manufactured by Advanced Propulsion Systems (APS), Oxnard California, in 1997 under the CALSTART initiative [Rohrauer, 2009 A]. In August 2008, UOIT acquired two of these electric buses hand built by APS, with a total production run of ≈ 30 units. They were used in the Grand Canyon as a shuttle service between the visitor parking lot and the sightseeing points on the South rim. When acquired by UOIT, the buses barely functioned and were rebuilt/repaired and subsequently licensed for operation in Ontario.

APS Bus Specifications

The buses have a unibody fibreglass composite design, with forward and rear sub frames for drive and steering axles mounts. As they have a fully electric design, all systems are powered from the Energy Storage System (ESS). Each bus accommodates 25 seated passengers and an additional 11 standing, not including the driver. The CALSTART consortium commissioned the development of the vehicles by Advanced Propulsion Systems (APS) in Oxnard, CA to support the original California Air Resource Board (CARB) Zero Emission Vehicle (ZEV) mandate [Rohrauer, 2009 A]. The ESS is comprised of 108 flooded SAFT NiCd modules of 6 V each. These are arranged into two parallel strings of 54 modules each for a nominal voltage

of 324 volts, and an amp-hour rating of 360 Ah. Maximum energy storage is thus 116 kWhr [360Ah x 324V].

Each bus has an air-bag suspension system with an on board 5 hp air compressor. Power steering and power brakes are electric over hydraulic with a direct coupled mechanical backup system for steering and a 12 V backup hydraulic pump for braking. Cabin heating is comprised of two 1.8 kW resistive heaters mounted mid ship, and a 3.6 kW resistive heater mounted in the front defroster plenum. Of the approximately 29 units ever built by APS, only 3 units are known to be operational today. Figures 11 to 14 below show images taken during the construction of the buses for the Burbank Transit Authority. The buses physical specifications are listed in Table 5.

Figure 11, Axles and materials used to build the chassis for the vehicles.
(from [APS Bus])

Figure 11 shows the material storage area at the building facility in Oxnard, CA. Drive axles, front axles, and brake drums can be seen [APS Bus].

Figure 12, Burbank Local Transit Staff members visit the factory in Oxnard
(from [APS Bus])

Figure 12 depicts the front sub-frame during assembly while customers visit the APS factory. The low profile sub-frame is designed for a low bus floor aiding in wheel chair access [APS Bus].

Figure 13, The chassis is moulded of fibreglass and plastic resin
(from [APS Bus])

Figure 13 shows the bus unibody design that relies on a fibreglass composite shell, notable for the expansive window openings [APS Bus].

Figure 14, Composite structure ready to be baked (cured).
(from [APS Bus])

Table 5, APS Bus Technical Design Specifications
[Rohrauer, 2009 A]

Mechanical Systems:
Average range: 115 km
Max range: 155 km
Top Speed: 72 kph
Vehicle weight: ~ 7570 kg (with driver), 11,000 kg GVWR.
Gearing: Single speed 2.5:1 chain-drive reduction [speed reducer] to the 5.6:1 differential. (14:1 motor to axle reduction)
Electrical System:
360 Amp-hr, 324 volts (nominal)
Batteries: 108 SAFT model STM 5.180 NiCd "mono-blocks" (Two parallel strings of 54, 180 amp-hr, 6 volt batteries)
Total energy capacity of batteries: 116 KW-hrs
Specific Energy: 55 Wh/kg, Specific Power: 175 W/kg
Design Life of Batteries: >2000 cycles at 80% DOD (~300,000 km)
Electric Motor/Drive: Rexroth Indramat, 68 KW peak, 3 Φ digital control vector drive
Battery charger: 75 KW, 3 phase, 440 volts input; recharge time: ~3 hrs.

Timing and Milestones

First Inspection:

The buses were purchased by UOIT from a facility in Hingham near Boston MA, after having resided in storage for a number of years on the South rim of the Grand Canyon. The new owner had acquired the vehicles from a government auction and was in the process of planning their dismantling for sale as parts. The SAFT STM 5.180 NiCd "Mono-blocks" cells are no longer in production; there is significant demand for these units, and are currently selling for approximately ≈$500/ea (used). We were successful in securing a provisional purchase through the hard work of Dr. Rohrauer who negotiated a deposit, transport to Boston, and putting a hold on dismantling. The author performed the initial inspection on site, and verified that the battery systems were sufficient to prove functionality.

The severely depleted batteries were the first obstacle to overcome. A BRUSA NLG513 charger was programmed as a constant voltage source with current limiting. The initial voltage was set at 425 V, with current limiting to 8 A. The initial charge of 8 hours was sufficient to wake the batteries and energize bus systems, verify drive train, electrical support, brakes, and heating. A short test drive of the two buses ensued.

Figure 15, APS Bus in Hingham, MA.

Concurrently, Ontario Power Generation (OPG) was approached via UOIT's Advancement office (Mr. Clive Waugh) for sponsorship. The generous support of OPG enabled UOIT to purchase the buses and have them imported and shipped to the Oshawa campus. Immediately after they arrived, work was begun to re-commission the buses for Ontario public roads.

On the Road:

Several issues had to be resolved to restore the buses to fully operational status such as: tire replacement; refresh the NiCd modules; implement a "light" charger until the original 440 V 3 phase charger could be rebuilt and adapted to Canadian standards, and make the buses compliant with Ministry of Transportation Ontario (MTO) standards. A commercial transport repair facility in Oshawa performed the final mechanical safety inspections, and the buses were subsequently licensed. The following list summarizes the numerous modifications/repairs that were performed by the author in order to prepare the buses for operation, enabling the subsequent research described in this thesis:

- Remove/clean/test and re-install the battery packs.
- Replace defective tires, match tires on buses for wear and type.
- Rewire the velocity pickups on the speed reducers, connect to the DART systems.
- Calibrate the DART systems
- Rebuild one charger for Canadian voltages.
- Rewire the traction motors from Y to Delta for added power.
- Adjust/re-install automatic power doors for proper operation
- Replace inverter fans
- Remove and rebuild ventilation fans on battery compartments and traction motor
- Continuously maintain batteries by topping the electrolytes.
- Re-install the parking brake actuators.
- Add daytime driving lights to the bus; the drive ready status is used to energize the headlamps.
- Repair windshield washer pumps
- Install license plate lights.
- Change the oil in the speed reducer and differentials.

- Adjust the air suspensions levellers, replace/tighten leaking fittings.
- Numerous other tasks for cosmetic reasons.
- Acquire and repair/reprogram Eagle Pitcher Battery Cycler-Analyser.

Figure 16, APS Bus being proven on campus

Figure 16 shows the APS bus in operation following repairs. To increase the visibility of this initiative and promote the project's research, OPG commissioned a marketing company to "Wrap" one bus with an eye catching pattern. (Figure 17)

Figure 17, UOIT OPG Bus "Wrap"

The "Wrap" has several features of note: a large NEMA 5-15 cord end graphically represented on both sides; OPG and UOIT logos on all four sides of the bus, a tag line "THIS BUS FILLS UP AT THE PLUG"; and a short paragraph on the rear describing the goals of the project, Figure 18.

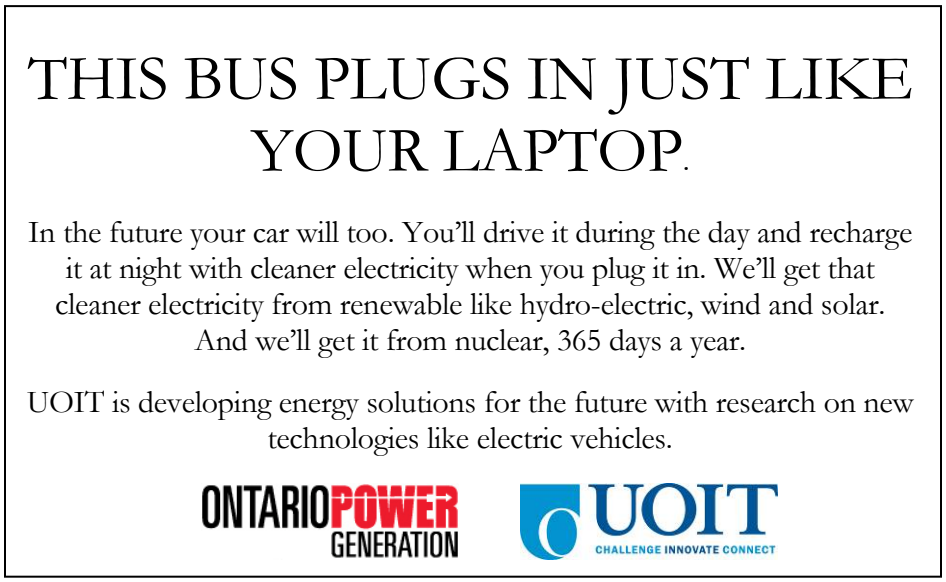

Figure 18, UOIT OPG Bus Caption

The second bus was "wrapped" with a different pattern, the NEMA 5-15 cord is again reproduced but on a light blue field, with a green grass border on the lower body panels. The tag line "UNIVERSITY OF ONTARIO INSTITUTE OF TECHNOLOGY, Developing tomorrow's transportation solutions today" is painted across the upper half, while sponsors' logos are placed on the lower half (Figure 19).

Figure 19, UOIT Shuttle Bus Wrap

The rear of the bus has the tag line: "UOIT has been selected as one of 17 universities in North America to compete in the EcoCAR Challenge, www.uoit.ca/ecocar" (Figure 20).

Figure 20, UOIT Shuttle Bus Graphics

Battery Maintenance:

The ESS was disassembled for maintenance; all batteries were inspected for mechanical damage, cleaned and tested with a fixed DC load, or an automated battery tester: Eagle Pitcher Model # MSD 970-1D. All the batteries passed tests, and the average capacity remaining was observed to be 55 kWh, or 49% of the original capacity. Internal battery resistance was measured, and the range was observed to vary from 1 to 77 mΩ, with an average of 2.3 mΩ. (This is due to differing states of health of modules across the ESS). Aggregate internal resistance of the ESS is calculated to be 65 mΩ from the individual measurements (Figure 21, Figure 22, Figure 23). The total resistance including cables and connections was observed to be 150 mΩ ±10 mΩ.

Figure 21, Bus ESS Maintenance in progress

Figure 21 shows the ESS module racks from one shuttle bus. The modules are waiting for capacity testing and battery terminal maintenance. The battery analyser apparatus is above and to the right in the background.

Figure 22, Battery Analyser Setup.

In Figure 22 the Eagle Pitcher 940-5D battery analyser is interfaced with a portable computer for data logging. Figure 23 illustrates the Eagle Pitcher battery analyzer running the MSD Computer Interface program to monitor parameters, and log them to sequential text files. This interface was used to log all the module tests and analyze the data for module health and internal resistance.

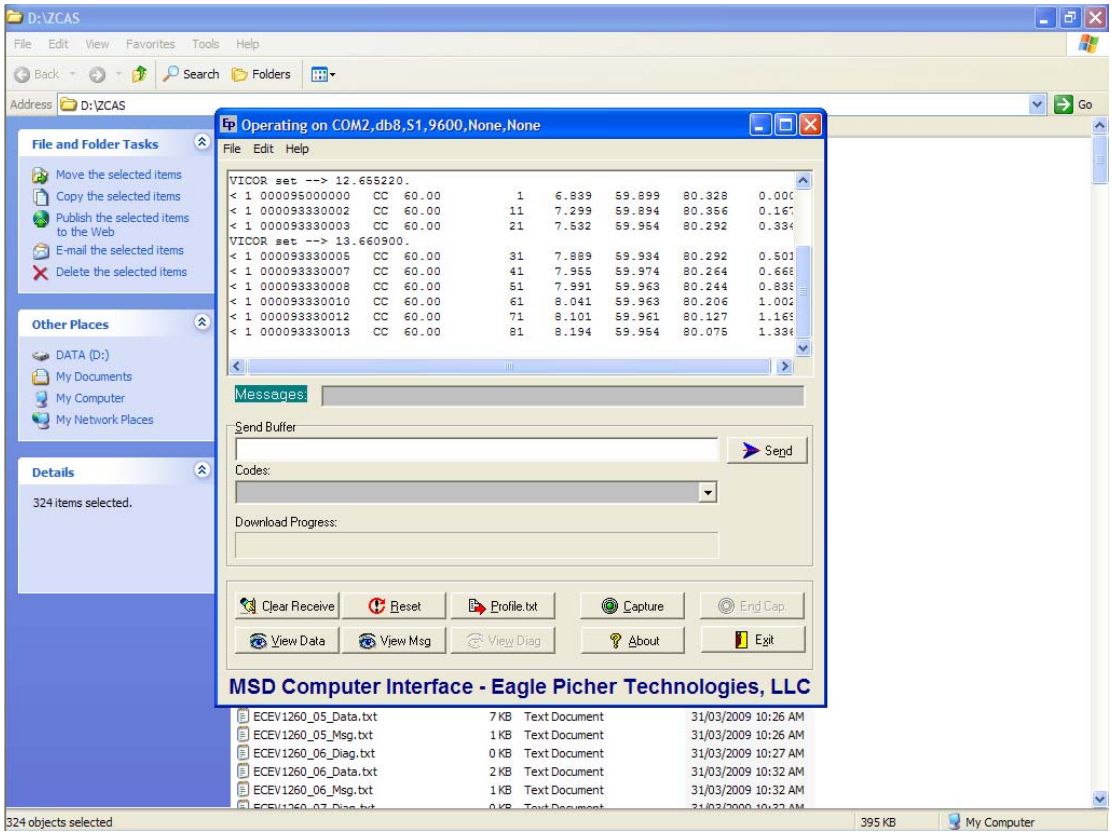

Figure 23, Battery Analyzer Data Logging application screen capture.

Conclusion

The APS Buses were acquired and commissioned for our study over the period of one year; once maintenance, inspections, and licensing were done data collection was started. Once the buses operated satisfactorily, they were ready for further study. Proceeding from the commissioning stage towards field trials and data collection was accomplished through 2008-2009.

Chapter 5

VEHICLE PERFORMANCE SIMULATION

Summary

The previous chapter provided an overview of the electric vehicles which were the primary object of the present research, including the considerable efforts needed to make them roadworthy. The present chapter describes how the data acquired through field trials was used to model the electric buses in Powertrain Simulation Analysis Toolkit (PSAT) so that their operational performance could be compared to diesel vehicles of similar physical size.

Introduction

In this chapter the data acquisition apparatus, and the mathematical model of the bus is described. A data acquisition trial was conducted, and the data was correlated with a model constructed in a software package called Powertrain System Analysis Toolkit (PSAT). As will be seen later, satisfactory correlation between the model and actual performance data was established.This was then used to predict energy usage and performance on a standard bus route. Finally, energy consumption of the APS electric bus was compared, concurrent with a diesel bus also modelled in PSAT and run over the same driving profiles.

Performance Data

Actual Performance Acquisition:

The APS electric buses were acquired with an energy data acquisition system that logs Voltage, Current, and Forward/Regenerative Power during a trip, as well as Charge Power input at the end of the cycle. The systems are able to log speed, and distance. As received by UOIT, this function was not wired into the Data Acquisition and Reporting Toolkit (DART) Energy Meter [SBETI, 1997]. An initial task was to connect the DART system to the odometer pulses from the traction inverter module, then calibrating the DART distance and velocity calculations. A GPS receiver positioned at the front of the bus was used to verify and calibrate both the speedometer and the DART system. The system sends a serial data stream three

times per second containing pertinent operational data. Figure 24 below illustrates the data packet:

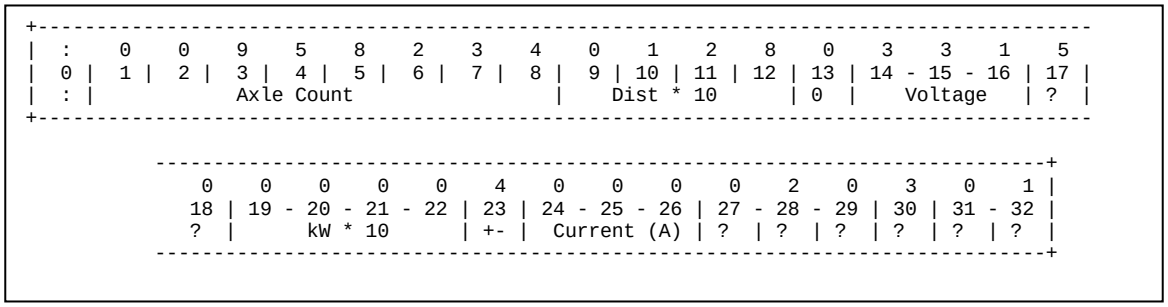

Figure 24, DART Data Packet

Along with a GPS receiver, an application to parse both GPS NMEA data and DART data was written. This accomplished the display of both data streams for cross-verification and logging to text files with date/time stamps. Figure 25, shows three sample text lines from the GPS receiver, a Holux M-1000 32 Channel Bluetooth GPS Receiver.

```
$GPGGA,225405.000,4356.2957,N,07853.4110,W,1,7,1.24,147.6,M,-35.3,M,,*66
$GPRMC,225405.000,A,4356.2957,N,07853.4110,W,0.30,125.07,231108,,,A*73
$GPVTG,125.07,T,,M,0.30,N,0.55,K,A*3F
```

Figure 25, GPS NMEA Data Packet, with longitude, latitude, speed and elevation encoded.

To log the data, a program was developed in Microsoft Visual Studio 2008 by the author. The goal was to log the data in sequential text files while synchronizing GPS and DART data streams. It was desired to allow easy customization of port addresses and parameters, while logging data from two discrete serial ports (DART on COM1, and GPS on COM5). Separate serial data stream windows showing the characters as they are received on the respective ports, and convenient buttons for connection and data logging, were implemented. Code listings are in Appendix A.

PSAT Model:

For model development and simulation, Powertrain System Analysis Toolkit (PSAT) V6.2 SP1, was used. A highly renown software tool developed by Argonne National Laboratory, it is used for evaluating vehicle performance and estimating tailpipe emissions. Using look up

tables of torque, speed, and efficiency maps of vehicle components, it then simulates the vehicle model through defined drive cycles to predict dynamic performance and fuel economy. Figure 26 shows the drivetrain configuration as modeled in PSAT with component specifications listed in Table 5 and APPENDIX B. The PSAT models values are listed in appendices B and C. From Figure 26, the components illustrated are described as follows:

- ESS: 2P54S, 180 Ah, 5 cell, 6 V, NiCd, 324 V
- Motor: induction, 3Φ, 32 kW nominal, 68 kW peak, ≈90% efficiency
- Torque Coupling: 2.5:1 chain drive
- Differential: ratio 5.8:1
- Wheels: number: 4, mass: 100 kg, radius: 0.37 m
- Vehicle: mass: 7570 kg
- DC/DC: inverter for 12 V electrical accessory bus
- Electrical Accessory: fixed load 2 kW

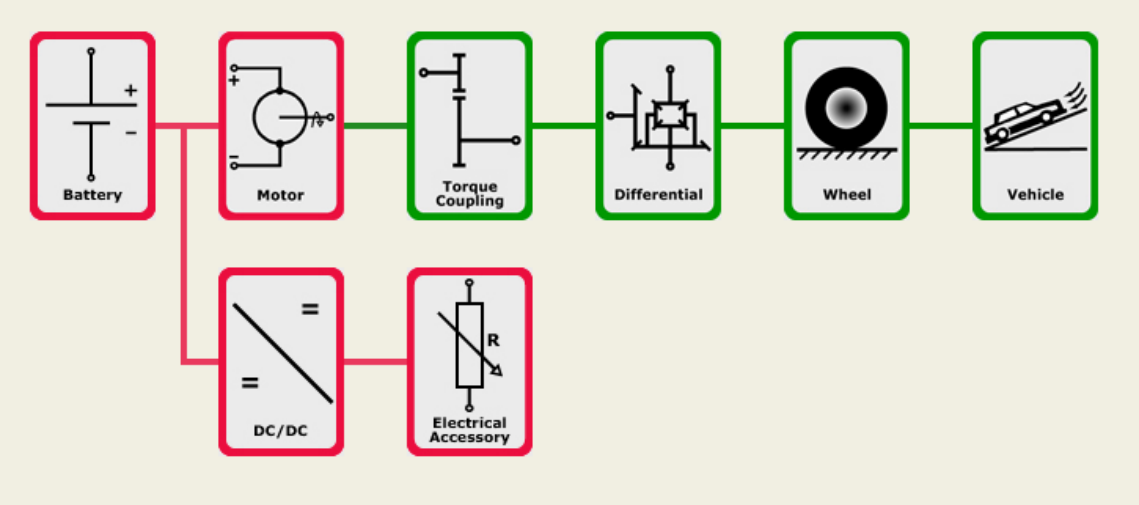

Figure 26, PSAT Model for APS Bus

Model Limitations and Sensitivities

Results from the PSAT model differ from the real world experimental data due to a number of simplifying assumptions. For example, in the computer model, the motor data is structured from dynamometer runs where tests are essentially taken at steady state operating points. These were translated into three dimensional torque and efficiency maps. External conditions

such as ambient humidity, temperature, barometric pressure, motor temperature rise rate, ESS temperature are generally static in the modeling, not necessarily identical to what is representative in field trials. Modeled transmission performance is influenced by operating temperature and the accuracy of the sub-models. Also, quasi steady state driving modeling does not account for real world energy losses associated with changing friction coefficients on the road. Road surface deflections (damper losses), wind effects, including the influence of headwind yaw angle on drag, and especially terrain elevation changes for vehicles operating under real conditions further influence the loss in accuracy of the predictions.

The simulations show that tire rolling resistance data and vehicle curb weight have a strong impact on the vehicle performance. As passenger and cargo weight are added, the acceleration rate is decreased. Tire rolling resistance affects the vehicle's energy consumption significantly [Stone, Ball, 2004]. For low speed commercial vehicles this resistance force accounts for at least 70% of the resistance force the vehicle has to overcome at its typical operating speed. If one considers rolling friction and aerodynamic drag and disregards elevation changes in the total resistance to motion, then aerodynamic drag and rolling friction are the principal contributing factors (Equation 4). As the speed of the vehicle grows, aerodynamic friction eventually becomes the main contributing factor. For small vehicles, this speed is much lower than for industrial transports where rolling resistance is the main form of drag [Genta, 1997].

$$Tractive\ Force\ F_T = F_{Rolling\ friction} + F_{aerodynamic\ drag} + F_{elevation}$$
$$Tractive\ Force\ F_T = C_{rr} mg \cos\alpha + \frac{1}{2}\rho V^2 A C_d + mg \sin\alpha$$

Equation 4, Tractive Forces (Steady State)
[Genta, 1997]

Total Tractive Forces

The speed capacity of the vehicle is bounded by several factors: available power output of the prime mover, rolling friction, aerodynamic friction, and forces due to elevation changes. In Equation 4, the total steady state tractive forces exerted on the vehicle against its motion are the rolling friction, the aerodynamic friction and change in elevation. Data from the shuttle bus was used to calculate the theoretical tractive forces, as illustrated in Figure 27. For the rolling resistance, the tire rolling resistance coefficient was calculated by performing a pull test on level

ground. The average pull force was recorded as 833.9 N unloaded; the pull force with a loaded bus was projected from this data to 1241.4 N.

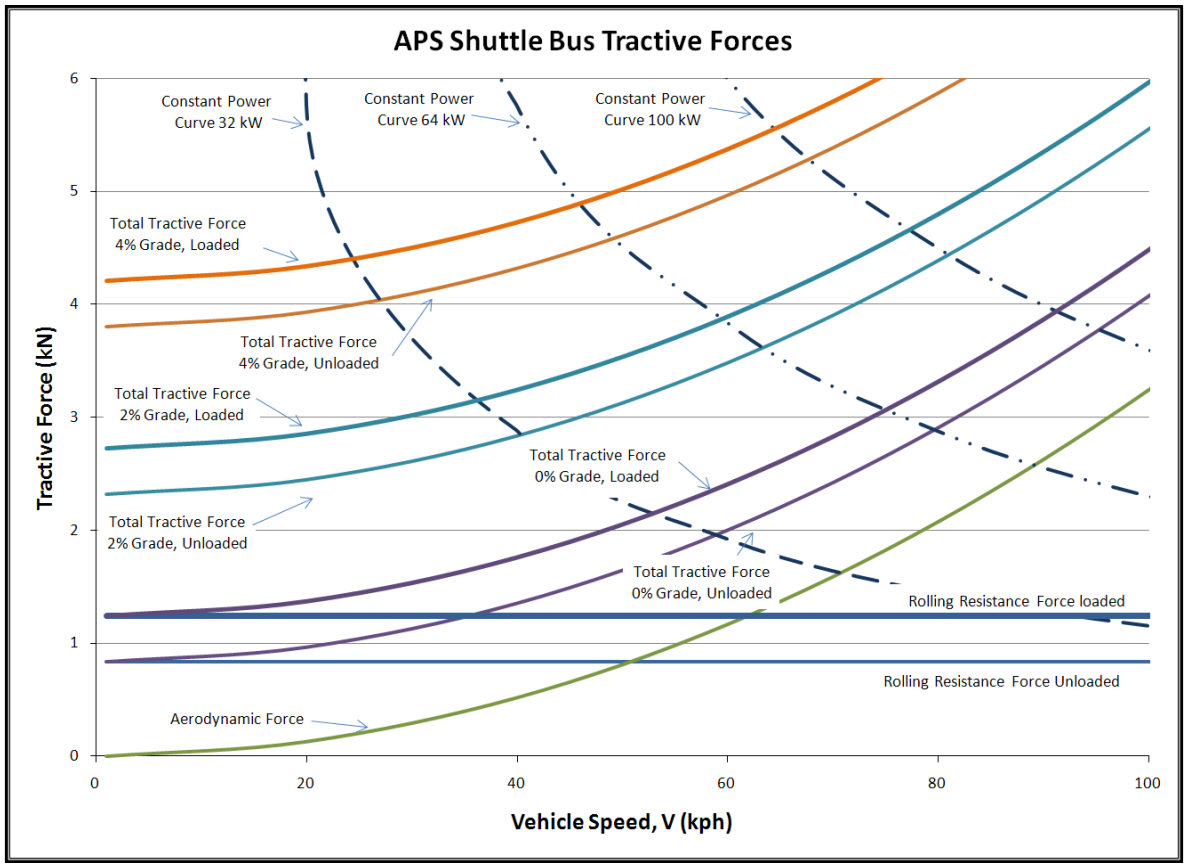

Figure 27, Road Drag Curves for APS Shuttle Bus

(Based on Equation 4, and the bus physical data for a range of speeds and grades)

In Figure 27, tractive forces are plotted for different speeds and grades. Superimposed are the constant power curves for three different levels of Powertrain output: 32, 64, and 100 kW. Where the Tractive Force curve intersects the constant power curve the maximum speed of the vehicle can be predicted. When the APS bus is operated at its maximum power output of 68 kW (DC power input to inverter from batteries as indicated by DART system), the maximum speed on level road is theoretically 82 km/h, and at a 4% grade 55 km/h. Heat buildup prevents continuous drivetrain operation at 68 KW. For sustained use, the maximum sustained speed at a 4% grade is 25 km/h.

Modelling Strategy:

In a field data run on a return trip from the North Oshawa to Downtown Oshawa, energy, speed, and elevation were recorded. The speed over time data was converted into a driving profile for PSAT (Figure 28). The APS Bus parameters were entered into a PSAT mathematical model and run with the driving profile from the recording. This process was accomplished to perform a correlation of the PSAT model with the field results. As seen in Figure 30, the PSAT results compared to the field data provided a reasonable comfort level to further employ the PSAT model of the electric bus in order to compare its performance to other vehicles.

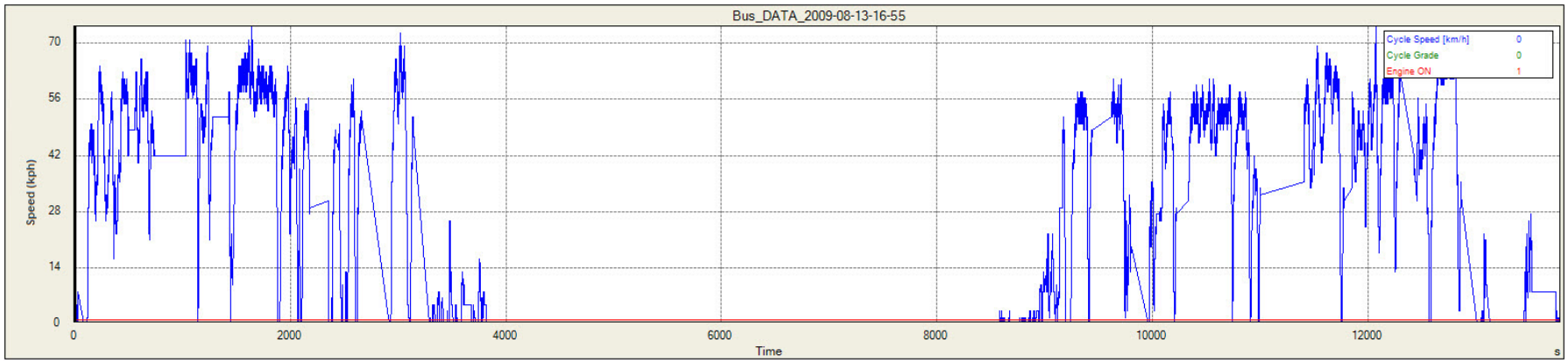

Figure 28, Simulation Driving Profile

The field trials were compiled and converted for simulation in PSAT see Figure 28. Therefore this driving profile applies to both field data and mathematical simulation. In Table 6 the results of the simulation are compared to the field trials. Simulations were run with the elevation profile and without, since results were not changed by the elevation data, this was removed from the driving profile to simplify the conversion.

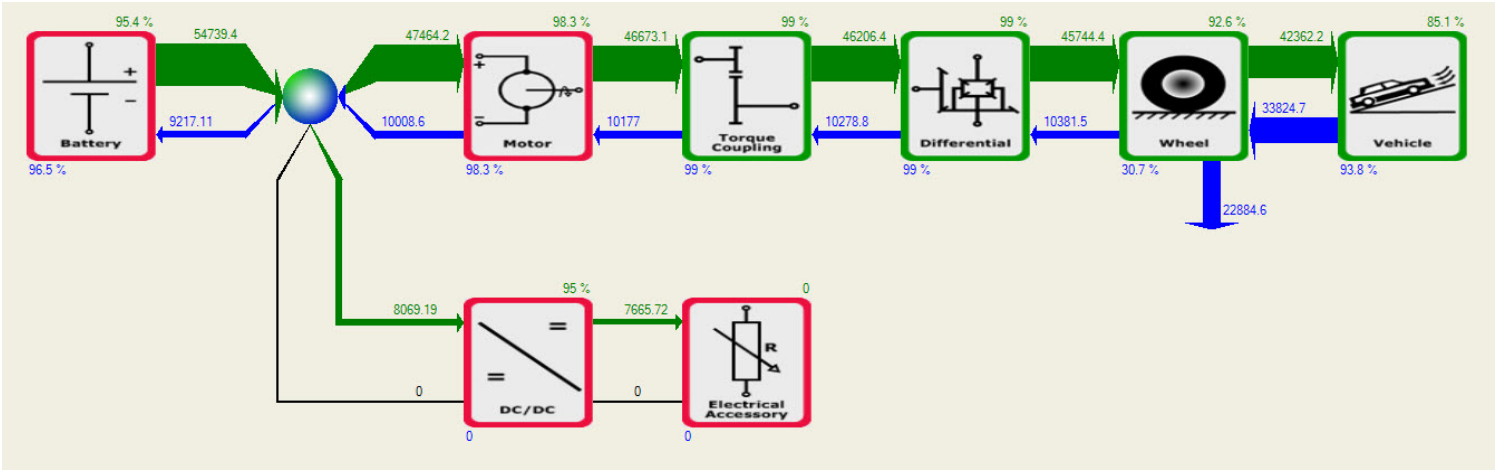

Figure 29, Simulation Energy Balance from PSAT

Description		Unit	Simulation # 14 (Run)
Results Interval		s	0 - 13798.3
Cycle			Bus_DATA_2009-08-13-16-55
Cycle distance		km	80.09
ELECTRICAL INFORMATION			
ESS			
Initial ESS SOC		%	100
Final ESS SOC		%	62.01
ENERGY SUMMARY			
Energy Unidirectional Loss ess	Energy Storage System	Wh	2980.34
Energy Unidirectional Loss mc	Motor Controller	Wh	959.51
Energy Unidirectional Loss tc_mc	Torque Coupling	Wh	568.48
Energy Unidirectional Loss fd	Final Drive	Wh	564.72
Energy Unidirectional Loss wh	Wheel Axle	Wh	26825.48
Energy Unidirectional Loss veh	Vehicle	Wh	8550.39
Energy Unidirectional Loss pc_accelec	Accesory Power Converter	Wh	403.46
Energy Unidirectional Loss accelec	Electrical Assesory	Wh	7665.72
Total Energy Unidirectional Loss (Components+Vehicle)		Wh	48518.1
Vehicle Unidirectional Output Energy in Inertia (during Acceleration and Deceleration)		Wh	-12.92
Input Energy from (Fuel + ESS#1 Net + ESS#2 Net + ESSHydra)		Wh	48502.76
Energy Balance Error		Wh	-15.35
Vehicle Forward Output Energy in Inertia (during Acceleration)		Wh	36059.46
Vehicle Aerodynamic Drag Energy Loss		Wh	8550.39
Vehicle Rolling Resistance Energy Loss		Wh	3940.91
Vehicle Grade Energy Loss		Wh	0
Total ESS Unidirectional Energy In		Wh	48502.76
Powertrain Energy Forward Path In (Fuel + ESS)		Wh	57398.01
Powertrain Energy Forward Path Out (at Wheel)		Wh	45744.49
Percentage Braking Energy Recovered at Battery		%	28.09
Percentage Braking Energy Recovered at Wheel		%	29.28
COMPONENT AVERAGE EFFICIENCIES			
Motor Bidirectional Efficiency		%	98.34
Motor Bidirectional Efficiency during Acceleration		%	98.33
Motor Bidirectional Efficiency during Deceleration		%	98.35
Powertrain Forward Path Efficiency		%	79.7
Powertrain Reverse Path Efficiency		%	85.66
Powertrain Bidirectional Path Efficiency		%	80.61
Powertrain Closed Loop Gain			2.51
STATISTICS			
Absolute average difference on vehicle speeds		km/h	0.47
Percentage of the time the trace is missed by 2mph		%	2.99
Total time the trace is missed by 2mph		s	412.5
Greatest percentage deviation from the trace in mph		%	366.95
At time		s	2349.7
Absolute deviation from the trace		km/h	23.32
At time		s	1030.2

The abs. dev. from trace is large, since the driveline power is limited and cannot accelerate quickly. Although, the % time the trace is missed is small.

Figure 30, PSAT, Bus Performance Simulation Results

A few of the results from Figure 30 are key to the analysis of vehicle operation; energy consumption; peak power demands; starting and ending SOC. The simulation energy consumption is 605.6 Wh/km, a result that is consistent with an electric vehicle of this size and mass. From the manufacturers' specifications with an ESS of 116 kWhr, a predicted range of 150 km is justified. The total power consumed during the simulation run of 3 hours and 50 minutes is 48.5 kWh, which corresponds to a third of the available energy from the ESS [Ye et al.].

Field Performance Results:

The simulation run was compiled from an actual run on Oshawa city streets while the bus performed several stops along the route from the UOIT Oshawa campus down Simcoe Street to the South end of the city and back to the campus. During the performance trial, the Electric Bus Data Logger program was running on a laptop capturing data from the DART Energy Monitor and the GPS receiver. As the data streamed in, it was compiled into a sequential text file. This was used for a performance analysis similar to the PSAT model. Results are summarized in Table 6. Note: Through battery maintenance and driving experiences, it was determined that the cells are presently at ≈55% of their original capacity, and driving experiments have shown that the energy consumed is 55 kWhr to "empty". This factor can explain some of the differences between the PSAT simulation results and the field test trial values of Table 6.

Table 6, Comparison of Simulation and Field Performance Data

Electric Bus Test Run				
13-Aug-09				
	PSAT Simulation	**Field Values**	**% Dev.**	**Units**
V initial	**367**	**362**	1.4	Volts
V final	**346**	**334**	3.6	Volts
Power Used	**48.502**	**48.786**	0.6	kWh
Power Recharge		**45.895**		kWh
Regenerative Power	**9.217**	**9.841**	6.3	kWh
Distance (imperial)	**50.0**	**55.0**	9.1	miles
Distance (metric)	**80.1**	**91.7**	12.6	km
Axle Pulse Count		**1129999**		count
Average Power	**522**	**532**	1.9	Wh/km
	836	**887**	5.8	Wh/mi
% regenerative	**17%**	**20%**	16	
Mass	**7570**	**7570**		kg
motor to axle ratio	**14**	**14**		
Tire Friction Coefficient	**0.004418**	**0.004418**		
Drag Coefficient CdA	**7**	**7**		m^2

The regenerative power is from Figure 29, the net power returned to the ESS.

Data Correlation

While the PSAT model does not allow for ambient wind, it does allow for: aerodynamic drag and road grade, the returned energy consumption correlated closely to the actual field data: (532.0 Wh/km) vs., 605.6 Wh/km from the PSAT model. Total power used is a little more complicated to simulate since the model does not account for parasitic asynchronous loads such as: door openings, wipers, or cabin heating. These losses are assumed in the steady accessory load. The field test displayed a power used of 48.8 kWh while PSAT predicted 48.5 kWh. Such results provide a high level of confidence that PSAT used as a route model energy consumption predictor for performance simulation is accurate. While GPS elevation was recorded, no effect could be discerned from either the field data or the PSAT simulation results. It is believed the cause could be circular routes, where the route terminates at the same point as the start; therefore the net elevation change is cancelled. Regenerative breaking also has an effect on road grade energy use where a portion of the kinetic energy is used to recharge the ESS.

Comparison to a Diesel Bus

Once the electric bus model was correlated with field data, this model was run against a typical bus route. This data was compared to an equivalent mass Orion bus using a diesel power plant, details in Figure 31. The route selected is a typical New York bus route that runs for 10 minutes and 0.98 kilometres. This route was chosen because of its maximum speed of 50 kph, which is easily within the electric bus performance envelope (Figure 32). In the simulation the diesel bus consumes 6.2 kWhr or 0.52 kg of diesel fuel, and the electric bus required 1.0 kWhr of electricity. The significant difference between the two vehicles can be explained by engine idling; the route has a 67% idle time while at stops whereas an electric vehicle has a distinct advantage in such cases.

At an approximate cost of $0.96/litre the energy cost of the Orion bus is $0.59, in the case of the electric bus estimated at $0.12 for 1.0 kWhr of electricity.

Description	Unit	APS Electric	Orion Diesel
Results Interval	s	0 - 600	0 - 600
Cycle		newyork_bus	newyork_bus
Cycle distance	km	0.87	0.87
THERMAL INFORMATION			
Engine			
Fuel economy	liter/100km		71.04
Fuel economy gasoline equivalent	liter/100km		79.02
Fuel mass	kg		0.52
HC emissions	g/km		0
CO emissions	g/km		0
NOx emissions	g/km		0
CO2 emissions	g/km		1899.4
ELECTRICAL INFORMATION			
ESS			
Initial ESS SOC	%	100	70
Final ESS SOC	%	99.24	61.15
ENERGY SUMMARY			
Energy Unidirectional Loss accmech	Wh		276.4
Energy Unidirectional Loss cpl	Wh		-27.22
Energy Unidirectional Loss gb	Wh		55.76
Energy Unidirectional Loss ess	Wh	37.34	15.34
Energy Unidirectional Loss gc	Wh		19.22
Energy Unidirectional Loss tc_gc	Wh		3.84
Energy Unidirectional Loss mc	Wh	82.59	
Energy Unidirectional Loss tc_mc	Wh	10.08	
Energy Unidirectional Loss fd	Wh	10.01	38.49
Energy Unidirectional Loss wh	Wh	492.62	1021.17
Energy Unidirectional Loss veh	Wh	25.9	37.77
Energy Unidirectional Loss pc_accelec	Wh	17.54	
Energy Unidirectional Loss accelec	Wh	333.33	166.67
Energy Unidirectional Loss eng	Wh		4534.67
Total Energy Unidirectional Loss (Components+Vehicle)	Wh	1009.42	6142.09
Vehicle Unidirectional Output Energy in Inertia (during Acceleration and Deceleration)	Wh	0.68	60.84
Input Energy from (Fuel + ESS#1 Net + ESS#2 Net +	Wh	1010.22	6202.95
Energy Balance Error	Wh	0.8	60.86
Vehicle Forward Output Energy in Inertia (during	Wh	726.14	988.69
Vehicle Aerodynamic Drag Energy Loss	Wh	25.9	25.9
Vehicle Rolling Resistance Energy Loss	Wh	31.1	353.65
Vehicle Grade Energy Loss	Wh	0	0
Engine Fuel Unidirectional Energy	Wh		6129.83
Total ESS Unidirectional Energy In	Wh	1010.22	73.12
Powertrain Energy Forward Path In (Fuel + ESS)	Wh	1181.57	6206.5
Powertrain Energy Forward Path Out (at Wheel)	Wh	758.4	1191.01
Percentage Braking Energy Recovered at Battery	%	30.51	0
Percentage Braking Energy Recovered at Wheel	%	33.72	
COMPONENT AVERAGE EFFICIENCIES			
Engine Bidirectional Efficiency	%		26.24
Generator Bidirectional Efficiency	%		85
Transmission Bidirectional Efficiency	%		95.87
Motor Bidirectional Efficiency	%	92.31	
Motor Bidirectional Efficiency during Acceleration	%	92.22	
Motor Bidirectional Efficiency during Deceleration	%	92.63	
Powertrain Forward Path Efficiency	%	64.19	19.19
Powertrain Reverse Path Efficiency	%	71.64	0.08
Powertrain Bidirectional Path Efficiency	%	65.44	18.97
Powertrain Closed Loop Gain		1.19	0.19
OTHER INFORMATION			
Engine			
Weight Specific Fuel Consumption Gas Eq. (WSFC)	liter/100km/ton		8.9
Mass of fuel needed to travel 320 miles	kg		305.46
STATISTICS			
Absolute average difference on vehicle speeds	km/h	0.73	0.76
Percentage of the time the trace is missed by 2mph	%	8.4	8.62
Total time the trace is missed by 2mph	s	50.4	51.7
Greatest percentage deviation from the trace in mph	%	62.37	87.24
At time	s	15.5	555.5
Absolute deviation from the trace	km/h	15.06	16.58
At time	s	333	79

Fuel comsumption number used for comparison

Only the Diesel bus has CO2 emmisions at the point of use. But, electric bus emmisions the from power generation can be calculated as: 191 g CO2. Where the Canadian Electricity average is 189 g CO2/kWhr.

Comparative Energy use: The two vehicles exhibit a 6x factor in energy use, diesel use more energy than electric

The EV bus electrical energy consumption for trip. 1010.22Wh/0.87km = 1161 Wh/km

Figure 31, Electric Bus Consumption Compared to an Orion Diesel Bus

Graph | Simulation Statistics

Cycle Time	600	sec	Distance	0.98364	km

	Maximum	Average	Standard Deviation	Unit
Speed	49.28	5.892	10.4219	km/h
Acceleration	2.7556	1.1614	0.8273	m/s2
Deceleration	-2.0444	-0.66869	0.55282	m/s2

	Number	Frequency	Duration	Percent of Cycle
Stop	11	0.011182903	404	67.333333
		stop / km	seconds	%

Figure 32, New York Bus Route Statistics

Analysis and results

This study clearly illustrates that an electric bus has far superior energy consumption characteristics compared to a similarly sized diesel bus, especially for an urban route as chosen. As shown, regardless of the ESS capacity, the energy budget for the electric bus is from 1158 to 1404 Wh/km under average running conditions. This result allows one to estimate cost at $0.15/km for an energy cost of $0.12/kWh. Allowing for battery charging efficiency, then the cost is ≈$0.34/km with a 45% efficiency charging system (as at present). The poor charging efficiency is reflected by the low level of technology used by the present charger, a simple 3 phase Silicon Controlled Rectifier (SCR) configured as a current controller. This charger has no filtering nor power factor correction implemented. Typical chargers employing DC/DC high frequency switching designs achieve ≈92% efficiency, instigate power factor correction, and effectively lower the measured power use. The NiCd cell's charge acceptance efficiency is ≈80%, this would result in a combined efficiency of ≈72% for a modern charger. Commensurate reductions in energy use to ≈$0.21/km are expected with a charger upgrade to a high frequency switching design with power factor correction.

Using an estimated cost of $0.96/litre for road taxed diesel, and an average fuel consumption of 71.0 L/100km (from the PSAT simulation, Figure 31), the expected fuel cost of operating the diesel bus of this study is $0.68/km. In other words, the diesel bus operating costs appear to be approximately three times that of a comparatively sized electric bus. Additionally, the electric bus contributes to negligible Green House Gas (GHG) emissions compared to fossil fuels if charged in the Canadian electrical energy mix. [Canadian Federal Government, 2007]

However, ESS cell replacement costs are not factored into this short operating cycle. A complete study would also factor maintenance along with depreciation.

GHG Emissions

The Canadian electrical energy generation emits GHG dependent on the type of generating plant. The CO_2 eq. produced by the electrical generating system is significantly different than in the USA and other parts of the world.

Table 7 shows the CO_2 that would be produced by the different provincial electrical generating systems for the New York bus route driving profile on a grams CO_2 eq. /km basis, for the electricity used to recharge the bus at the end of the run. The province of Quebec would only generate 1.8 CO_2 eq., while for Nova Scotia 774.1 g CO_2 eq. would be expected [Canada 2010], [Environment Canada].

Table 7, CO_2 eq. / kWhr for different Provincial Generating Systems

Electric Bus CO2 eq. from Charging (g CO_2 eq. for New York Bus Route)	
Province	**g CO_2 eq. for New York Bus Route**
Alberta	720.9
British Columbia	24.3
Manitoba	18.9
New Brunswick	449.6
Newfoundland and Labrador	74.3
Nova Scotia	774.1
Ontario	181.7
Quebec	1.8
Saskatchewan	676.9
Canadian Weighted Average	189.3

(compiled from [Canada 2010], [Environment Canada])

The PSAT predicted energy consumption of 71.04 L/100 km for the diesel bus, has a strong correlation to published data. The Transportation Energy Data Book, Edition 28, 2009,

indicated a fuel consumption of 70.2 L/100 km for all transit buses in the US in 2007 [Davis, et al., 2009].

Conclusion

Electric buses have a far superior energy consumption characteristics compared to a similarly sized diesel bus. As shown in this chapter, regardless of the ESS capacity, the energy budget for the electric bus is from 931 to 1132 Wh/km (Table 8). This result allows one to estimate cost at \$0.12/km for an energy cost of \$0.12/kWh. Allowing for battery charging efficiency (80%) [Buchmann, 2001], then the cost is \$0.34/km with a 45% efficiency charging system and \$0.21/km with a modern charger. Using an estimated cost of \$0.96/litre for road taxed diesel, and average fuel consumption from the PSAT model of 71.04 L/100 km, the fuel cost of operating the diesel bus in this study works out to \$0.68/km. In other words, the diesel bus energy operating costs appear to be approximately three times that of comparatively sized electric bus. Additionally, the electric bus contributes negligible GHG emissions compared to fossil fuels in the Canadian electrical energy mix of 189.3 g CO_2/kWhr (see Figure 31) [Canadian Federal Government, 2007].

The next chapter models the electric bus with an alternate ESS technology and factors the price of the ESS into the operating cost of the vehicle.

Chapter 6

ENERGY STORAGE SYSTEM OPERATIONAL COSTS

Summary

The previous chapter provided an analysis of the energy performance of an electric bus compared to a diesel version using PSAT to model the vehicles. The present chapter assesses the cost of operation of an electric bus for energy including the ESS life costs against the running costs of a similar diesel bus.

Introduction

While the energy consumption cost of an electric bus is lower than a comparable diesel bus, a significant portion of the operating expense is invested into the cost of the Energy Storage System (ESS). As the ESS is repeatedly charged/discharged the properties of the cells change, this change is reflected as a degradation of the capacity in the cells to store charge. This is normally measured by the BMS and indicated as the State of Health (SOH). Previously different cell technologies were considered for performance and cost; here the data is used to calculate the operational cost of the electric vehicle for energy and the amortized cost of the ESS.

Electric Bus Model

The electric bus is modelled with an alternate battery technology, since in Table 3 the HiPower HP-50160282 had the lowest cost of ≈$164/MWhr for its life cycle, this is the basis chosen with the an ESS of the same capacity (360Ah), but using the lighter LiFePO cells. In the APS electric bus the SAFT NiCd modules have a total mass of 2505 kg; the new LiFePO cells would have a mass of 1564 kg. This difference of 941 kg is deducted from the electric bus model mass along with changes to the cell's internal resistance characteristics. The new bus model was run in PSAT and the summary results are shown in Figure 33.

Description	Unit	NiCd ESS		$LiFePO_4$ ESS	
Results Interval	s				
Cycle		newyo...	newyo...	newy...	newy...
Cycle distance	km	0.87		0.89	
ELECTRICAL INFORMATION			Full Load		Full Load
ESS					
Initial ESS SOC	%	Empty	100	Empty	100
Final ESS SOC	%		99.14		99.99
ENERGY SUMMARY					
Energy Unidirectional Loss ess	Wh	37.34	45.13	1.04	1.32
Energy Unidirectional Loss mc	Wh	82.59	103.35	76.06	97.77
Energy Unidirectional Loss tc_mc	Wh	10.08	11.74	9.4	11.38
Energy Unidirectional Loss fd	Wh	10.01	11.66	9.34	11.3
Energy Unidirectional Loss wh	Wh	492.62	586.01	457.17	563.19
Energy Unidirectional Loss veh	Wh	25.9	22.27	26.96	23.61
Energy Unidirectional Loss pc_accelec	Wh	17.54	17.54	17.54	17.54
Energy Unidirectional Loss accelec	Wh	333.33	333.33	333.33	333.33
Total Energy Unidirectional Loss (Components+Vehicle)	Wh	1009.42	1131.03	930.85	1059.44
Vehicle Unidirectional Output Energy in Inertia (during Acceleration and Deceleration)	Wh	0.68	0.24	0.58	0.6
Input Energy from (Fuel + ESS#1 Net + ESS#2 Net + ESSHydra)	Wh	1010.22	1131.8	931.14	1060.09
Energy Balance Error	Wh	0.8	0.76	0.29	0.65
Vehicle Forward Output Energy in Inertia (during Acceleration)	Wh	726.14	847.07	677.3	820.25
Vehicle Aerodynamic Drag Energy Loss	Wh	25.9	22.27	26.96	23.61
Vehicle Rolling Resistance Energy Loss	Wh	31.1	38.33	28.53	36.54
Vehicle Grade Energy Loss	Wh	0	0	0	0
Total ESS Unidirectional Energy In	Wh	1010.22	1131.8	931.14	1060.09
Powertrain Energy Forward Path In (Fuel + ESS)	Wh	1181.57	1341.3	1088.79	1264.48
Powertrain Energy Forward Path Out (at Wheel)	Wh	758.4	885.17	707.74	856.66
Percentage Braking Energy Recovered at Battery	%	30.51	30.12	30.34	30.39
Percentage Braking Energy Recovered at Wheel	%	33.72	33.32	33.61	33.6
COMPONENT AVERAGE EFFICIENCIES					
Motor Bidirectional Efficiency	%	92.31	91.78	92.4	91.96
Motor Bidirectional Efficiency during Acceleration	%	92.22	91.6	92.34	91.82
Motor Bidirectional Efficiency during Deceleration	%	92.63	92.4	92.61	92.47
Powertrain Forward Path Efficiency	%	64.19	65.99	65	67.75
Powertrain Reverse Path Efficiency	%	71.64	75.73	70.68	75.91
Powertrain Bidirectional Path Efficiency	%	65.44	67.66	65.97	69.18
Powertrain Closed Loop Gain		1.19	1.32	1.2	1.39
STATISTICS					
Absolute average difference on vehicle speeds	km/h	0.73	1.14	0.62	1.01
Percentage of the time the trace is missed by 2mph	%	8.4	11.37	7.45	10.1
Total time the trace is missed by 2mph	s	50.4	68.2	44.7	60.6
Greatest percentage deviation from the trace in mph	%	62.37	71.46	58.41	69.26
At time	s	15.5	15.5	15.5	15.5
Absolute deviation from the trace	km/h	15.06	17.72	13.88	17.09
At time	s	333	333	333	333

Figure 33, Electric Bus Simulation with a LiFePO and NiCd ESS

The electric bus simulation was run with different configurations using NiCd and $LiFePO_4$ for the ESS; unloaded and fully loaded with passengers for both cell technologies. The full passenger load was estimated to be 37 persons with a mix of 40% male, 40% female and the remainder as children, using Transport Canada passenger specifications this additional load is estimated to be 2700 kg [Gaudreau, 2010]. The results are tabulated in Table 8.

Table 8, Electric Bus Energy Consumption

Electric Bus Energy Consumption (kWhr/km)			
ESS cell Type	**Load:**	**Empty**	**Full**
	NiCd:	1010	1132
	LiFePO:	931	1060

Table 8 shows the advantage gained by the lighter ESS composed of LiFePO cells for the same energy capacity. The mass saving of 941 kg changed the energy consumption from 1010 to 931 Wh/km (Unloaded).

Using the predicted cycle count of Table 3 for the HiPower cell, 3000 at a 70% DOD, and a capital cost of $1.10/Ah for the cells, the estimated price for the cells before BMS and installation is ≈$47,520 or $15.84/cycle (excludes freight, taxes/duties). The estimated range is 89 to 126 km per full cycle for the electric bus with LiFePO cells (operating radius ≈ 45 km). Then the cost of the cells per kilometre is ≈$0.17/km. Added to the energy cost the total is ≈$0.51/km, the diesel fuel cost of the bus in the previous chapter was $0.68/km. The simple electric bus energy cost including ESS cells is approximately ¾ of the diesel bus. If the charging system were to be improved the predicted total energy cost drops to ≈$0.38/km, a ≈25% improvement. These calculations are performed for NiCd cells with a ≈80% charging efficiency. As lithium cells typically have ≈95% charging efficiency, the energy cost per kilometre drops to ≈$0.33/km. This amounts to about half the operating cost per km of diesel.

Conclusion

While the cost of the ESS technology is more significant to the operation of the electric bus than the cost of energy, the combined cost of cells and electricity is still advantageous compared to a diesel bus. The combined electricity and ESS cell cost of the electric bus is estimated ≈$0.33/km, while the diesel bus carries a fuel cost of $0.68/km. Fuel costs are expected to rise much more rapidly than electricity prices, while battery costs are predicted to approach $250.00/kWhr [Santini] along with higher cell cyclic life. Thus the operating cost advantages are expected to continue growing over time. Other costs related to vehicle operation, such as: drivers; depreciation; vehicle maintenance; insurance; capital; and licensing are not considered to simplify the estimates.

Future cost consideration must also be given for energy, as oil price is trending up at a higher rate than electricity prices, see Figure 34. In Canada electricity prices have been stable for several years, see Figure 35 [Canada 2001]. Further, electricity is produced from a much broader range of fuel/energy sources than petroleum; hence its price sensitivity to demand and supply is far less.

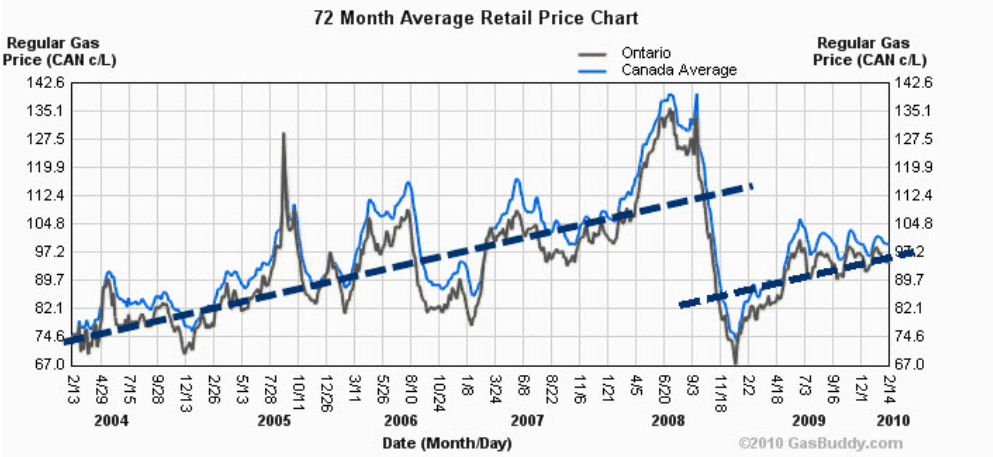

Figure 34, 72 Month Average Retail Price Chart with Tends
(modified from [72 Month Average Retail Price Chart])

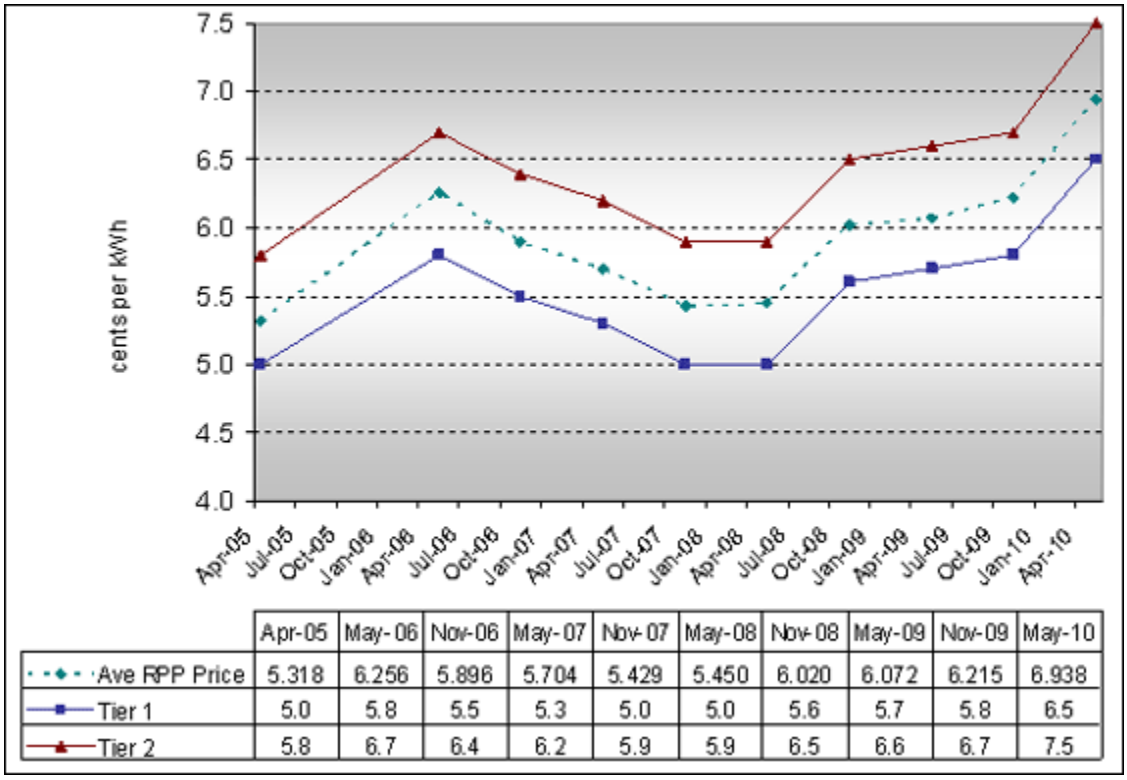

	Apr-05	May-06	Nov-06	May-07	Nov-07	May-08	Nov-08	May-09	Nov-09	May-10
Ave RPP Price	5.318	6.256	5.896	5.704	5.429	5.450	6.020	6.072	6.215	6.938
Tier 1	5.0	5.8	5.5	5.3	5.0	5.0	5.6	5.7	5.8	6.5
Tier 2	5.8	6.7	6.4	6.2	5.9	5.9	6.5	6.6	6.7	7.5

Figure 35, Regulated Price Plan Tiered Prices: Historical Snapshot

(from [Electricity Prices | OEB])

Chapter 7

SUMMARY AND CONCLUSIONS

The main conclusions emerging from the present work are:

This study illustrates the fact that an electric bus has far superior energy consumption and CO_2 generation characteristics compared to a similarly sized diesel bus. As shown in this study, regardless of the ESS capacity, the energy budget for the electric bus is from 931 to 1132 Wh/km (Table 8). This result allows one to estimate cost at $0.12/km for an electricity rate of $0.12/kWh. Allowing for battery charging efficiency, then the cost is presently $0.34/km with a 45% efficiency charging system; a modern charger would lower the cost to $0.17/km. Based on an estimated cost of $0.96/litre for road taxed diesel, and an average fuel consumption for all transit buses in the US of 70.2/100km (from the Transportation Energy Data Book, Edition 28, 2009) [Stacy, et al., 2009], the average fuel cost of operating the diesel bus of this study is $0.68/km. The diesel bus operating costs appear to be approximately 3 times more than a comparatively sized electric bus including charging. Additionally, the electric bus contributes to negligible GHG emissions compared to fossil fuels in the Canadian electrical energy mix [Canadian Federal Government]. Diesel bus CO_2 emissions were calculated to be 2183 g/km whereas the electric bus generated 272 g/km, a GHG reduction factor of 8.

The carbon footprint of electrical generation from legacy coal fired generators is >1,000 gCO_2eq/kWh [United Kingdom]; using power from this source to charge the electric bus would imply the generation of 1010 gCO_2eq/km, compared to 1899 gCO_2eq/km for the diesel bus, still better.

Buses are efficient people movers, the energy consumption per person for the electric bus is 30.6 Wh/person/km for a full load, versus 75 Wh/person/km for an electric sedan using 300 Wh/km. Electric bicycles typically achieve ≈24 Wh/person/km, and would be the lowest energy consumption motorized transport observed by the author.

The energy cascade for another form of electric vehicle, the hydrogen fuel cell (FC) bus has significant losses as the energy flows from generation to conversion and utilization. Only 25% of the input is available to the vehicle, whereas the battery powered electric bus has 90% of the input energy available for charging the ESS [Bossel][Larminie, and Lowry]. This gives the battery electric bus a significant advantage over the FC electric bus.

ESS cell replacement costs factored into operation indicate that the cost per kilometer is already less than diesel and the gap has a widening trend.

Powertrain System Analysis Toolkit (PSAT) is a valuable tool to estimate performance data on vehicles. The results are sufficiently accurate to provide a high level of confidence in predicting actual on-road performance.

Original contributions performed in the course of this work are:

Complete repair and maintenance of two APS electric buses to make them roadworthy in order to obtain authentic electric bus performance data.

Compilation of Table 3 from industrial sources in order to compare battery cells for energy density, dimensions, and expected energy performance.

Custom software for synchronous data logging of incompatible systems: GPS receiver and DART system. See Appendix A.

The implementation of a strategy for translating field test data into a PSAT driving profile.

Design of a strategy to contrast an electric bus with comparable diesel bus performance using PSAT.

Estimating basic per kilometre operating costs upon upgrading to the more effective lithium ion ESS available today.

Future Directions for Research and Commentary

It is difficult to estimate the financial cost of GHG emissions, although there is a strong trend to implement GHG emission reduction measures [Richer, 2008]. When "Carbon Taxes" materialize, GHG emissions can then be factored into the operational costs for fossil fuel use in both diesel and electric vehicles.

The cost of energy and ESS cells is considered in this work, a complete evaluation of the advantages of an electric bus would also consider all the operational issues of both vehicles. The diesel bus has significant maintenance and depreciation costs but these should be considered against the electric bus's respective operational costs for an inclusive estimate.

A computer model of a diesel bus was compared to the electric bus. An actual diesel vehicle of comparable dimensions to the electric bus should be instrumented. Energy consumption data would be directly related to the size of the vehicle, instead of aggregate consumption from the transportation study. Data collected from the diesel vehicle would provide a better comparison to the electric one.

Power input to the charging system should be more accurately measured. A power meter needs to be secured to measure the power input to the charging system. Currently a 70 kW charger (throttled to 30 kW by building limitations) is being used that requires 3 hours for a full ESS charge cycle. This charge rate was sufficient for satisfactory testing of the bus. For operation on a regular cyclic route the charger power would have to be restored. The poor efficiency of the present charger adds an un-necessary cost to the operation, a modern (high-efficiency) charger upgrade is needed.

From field trials the current SAFT NiCd cells have approximately 50% of their original capacity. In the event of a module failure, the modules cannot be sourced since the manufacturer has stopped production. This factor and continued research on electric vehicles steers one towards an upgrade of the ESS. Newer technology modules could be used to replace the ESS for a higher energy density design.

The current ESS does not have module level monitoring of the batteries, in the event of a module failure no indication is provided to the operator. A BMS with operator indication of module SOC and SOH would improve the operation and system safety.

As shown in Figure 27, the drivetrain power is sufficient for short trips between buildings, but insufficient for longer trips across the city where hills and +60 km/h traffic are encountered. The drivetrain (inverter, motor, gear reduction) should be replaced by a higher power system of approximately 120 kW, to make the bus useable on all secondary roads [80 kph].

The current suspension uses an air bag design with automatic adjusters, including a single shock absorber at each wheel. The original shock absorbers are in need of replacement.

The APS Bus was designed for the southern part of the US; our northern climate requires additional thermal isolation and outside air sealing from the elements. The electrically operated door is unreliable and weak; a more robust closing mechanism is needed.

Electrical resistive heaters are used for inside temperature control, these are sufficient at 0°C but do not comfortably heat the cabin in below freezing temperatures. Electric resistive elements use significant power from the ESS, reducing vehicle range as a consequence. A roof mounted thermal heat pump system could be used for a more comfortable cabin environment, with the electric resistive heaters to complement at lower temperatures.

Economic value estimates only include initial material costs; these have to be revised to include installation hardware, labour, shipping, overhead, tax and duties. Similarly, the electric bus is compared to the diesel CI bus only on the basis of energy inputs, a more thorough analysis would include all the operational costs for both vehicles such as: personnel, maintenance, depreciation, storage, licensing and insurance, and allowances for repairs.

REFERENCES

"*72 Month Average Retail Price Chart.*" Gas Price Historical Price Charts. Web. 23 Apr 2010. <http://www.gasbuddy.com/gb_retail_price_chart.aspx?time=24>.

"APS Bus." Advanced Propulsion Systems (APS) "*Burbank Local Transit Unveils Four New Electric Buses.*". Web. 7 Nov 2008. <http://www.ci.burbank.ca.us/blt/EVconstruct.htm>.

"Typical Voltage and Specific Gravity Characteristics of a Lead-acid Cell (constant-rate discharge and charge).." different types of photovoltaic systems. Web. 12 Apr 2010. <http://polarpowerinc.com/info/operation20/operation25.htm>.

Axsen, Jonn, Burke, Andrew, Kurani, Ken, "*Batteries for Plug-in Hybrid Electric Vehicles (PHEVs): Goals and State of Technology circa 2008*" Institute for Transportation Studies, University of CA, Davis, May 2008.

Beauregard, Garrett P. "prius_fire_fforensics.pdf." EV WORLD: The Future in Motion. ETEC, 26 Jun 2008. Web. 9 Mar 2010. <http://www.evworld.com/library/prius_fire_forensics.pdf>.

Bossel, Ulf. "The Hydrogen Illusion." *Cogeneration and On-Site Power Production* (2004): 55-59. Web. 14 Apr 2010. <http://www.efcf.com/reports/E11.pdf>.

Buchmann, Isidor. "*Can the lead-acid battery compete in modern times?*" *BatteryUniversity.com*. 2003-2005. CADEX, Web. 7 Mar 2010. <http://www.batteryuniversity.com/partone-6.htm>.

Buchmann, Isidor. *Batteries in a portable world*. 2ed. Cadex Electronics Inc, 2001. Print.

Canada 2001. *Canadian Electricity Trends and Issues*. Calgary, Alberta: Publications Coordinator National Energy Board, 2001. Web. 23 Apr 2010. <http://www.neb.gc.ca/clf-nsi/rnrgynfmtn/nrgyrprt/lctrcty/lctrctytrndssscnd2001-eng.pdf>.

Canada 2010. *Report on Energy Supply and Demand in Canada*. Ottawa: Statistics Canada, 2010. Web. 13 Apr 2010. <http://dsp-psd.pwgsc.gc.ca/collection_2010/statcan/57-003-X/57-003-x2008000-eng.pdf>.

Canadian Federal Government. *Electric Power Generation, Transmission and Distribution*. Ottawa: Minister responsible for Statistics Canada, 2007. Print.

Canadian Federal Government. *Electric Power Generation, Transmission and Distribution*. Ottawa: Minister responsible for Statistics Canada, 2007. Print.

Codecà, Fabio, Sergio M. Savaresi, and Giorgio Rizzoni. "On battery State of Charge estimation: a new mixed algorithm.." *17th IEEE International Conference on Control Applications Part of 2008 IEEE Multi-conference on Systems and Control San Antonio, Texas, USA*. (2008): Print.

Davis, Stacy C., Susan W. Diegel, and Robert G. Boundy. United States. *TRANSPORTATION ENERGY DATA BOOK: EDITION 28*. Oak Ridge, Tennessee: Center for Transportation Analysis Energy and Transportation Science Division, 2009. Web. 6 November 2009. <http://cta.ornl.gov/data/tedb28/Edition28_Full_Doc.pdf>.

Doerffel, Dennis, and Suleiman Abu Sharkh. "A critical review of using the Peukert equation for determining the remaining capacity of lead-acid and lithium-ion batteries." *Journal of Power Sources*. 152.2 (2006): 395-400. Print.

Fuhs, Allen E. *Hybrid vehicles and the future of personal transportation*. 1st ed. Boca Raton, FL, USA: CRC Press, 2008. Print.

Gaudreau, Michel. Canada. *Air Operator Weight and Balance Control Procedures Subparts 703/704/705 of the Canadian Aviation Regulations*. Ottawa: Transport Canada, 2010. Web. 20 Mar 2010. <http://www.tc.gc.ca/civilaviation/commerce/circulars/AC0235r.htm>.

Genta, Giancarlo. *Motor vehicle dynamics*. 1. 43. Singapore: World Scientific Pub Co Inc, 1997. Print.

Griffith, Paul, and Gleason, Gary. United States. *Eight Years of Battery-Electric Bus Operation at the Santa Barbara Metropolitan Transit District*. Santa Barbara: Santa Barbara Electric Transportation Institute (SBETI), 2000. Web. 14 Apr 2010. <http://sbeti.org/8_years.pdf>.

Hiro Energy, "Components and Devices." *HIRO Energy*. Web. 8 Mar 2010. <http://www.hiroenergy.co.jp/denchi.html#a_namari>.

Idaho National Laboratory . "Advanced Vehicle Testing Activity - Full Size Electric Vehicles." *Idaho National Laboratory*. 30 May 2006. Idaho National Laboratory, Web. 7 Mar 2010. <http://avt.inel.gov/fsev.shtml>.

Larminie, James, and John Lowry. *Electric Vehicle Technology Explained*. 1st ed. Chichester, West Sussex, England: John Wiley & Sons Ltd, 2003. Print.

Martinez, Carlos. "pwrt0207.pdf." AnalogZone. Intersil Corporation, 02 May 2005. Web. 9 Mar 2010. <http://www.analogzone.com/pwrt0207.pdf>.

Ontario, Canada. *Electricity Prices | OEB*. Toronto: Queens Printer for Ontario, 2008. Web. 26 Apr 2010. <http://www.oeb.gov.on.ca/OEB/Consumers/Electricity/Electricity+Prices>.

Peukert, Wilhelm "*Über die Abhängigkeit der Kapazität von der Entladestromstärke bei Bleiakkumulatoren*" Elektrotechnische Zeitschrift, volume 20, 1897, pp. 20–21.

Raman, N., Chagnon, G., Hafner, S., Nechev, K. , Romero, A., Saft, M. "*Development of High Power Li-Ion Battery Technology for Hybrid Electric Vehicle (HEV) Applications*", in: Proceedings of the 41st Power Sources Conference, June 2004, pp. 435–437.

Richer, Éric. Canada. *Government Delivers Details of Greenhouse Gas Regulatory Framework*. Ottawa: Environment Canada Media Relations, 2008. Web. 21 Mar 2010. <http://www.ec.gc.ca/default.asp?lang=En&n=714D9AAE-1&news=B2B42466-B768-424C-9A5B-6D59C2AE1C36>.

Ritchie, Andrew, Howard, Wilmont. "*Recent Developments and Likely Advances in Lithium-Ion Batteries*". Journal of Power Sources 162 (2006). Pp 809-812.

Rohrauer, Greg. "*Bus Flyer*." Print 26 Apr 2009.

Rohrauer, Greg. "*Thermal Management System Technology Development For Extended Range Electric Vehicles*." Grant application to Automotive Partnerships Canada Program. 14/07/2009

Santini, D.J. United States. *Cost-Effective PHEV Range: Battery Costs Versus Charging Infrastructure Costs*. Washington, DC: Argonne National Laboratory ("Argonne"). Argonne, 2010. Web. 7 Apr 2010. <http://cta.ornl.gov/trbenergy/trb_documents/2010/Santini%20Session%20538.pdf>.

SBETI. *A Performance Monitoring System for Battery-Electric Bus Operators, User's Guide*. Hardware Version 1.4. Santa Barbara, CA: Santa Barbara Electric Transportation Institute, 1997. Print.

Sony. "*Sony Lithium Ion Rechargeable Battery*." *Sony Battery*. Jun 2001. Sony Corp., Web. 8 Mar 2007. <http://www.sony.co.jp/en/Products/BAT/ION>.

Stone, Richard, and Jeffrey Ball. "*Automotive engineering fundamentals*." Warrendale, PA: Society of Automotive Engineers, 2004. Print.

United Kingdom. *Postnote*. London, UK: Parliamentary Office of Science and Technology, 2006. Web. 14 Apr 2010. <http://www.parliament.uk/documents/upload/postpn268.pdf>.

Vallese, Julie, and Scott Wolfson. United States. *Sony Recalls Notebook Computer Batteries Due to Previous Fires*. Washington, DC: Office of Information and Public Affairs, 2006. Web. 20 Mar 2010. <http://www.cpsc.gov/cpscpub/prerel/prhtml07/07011.html>.

Wang, J P, L Xu, J G Guo, and L Ding. "Modelling of a battery pack for electric vehicles using a stochastic fuzzy neural network." *Proceedings of the Institution of Mechanical Engineers, Part D: Journal of Automobile Engineering*. 223.1 (2009): 27-35. Print.

Weast, Robert C., *Handbook of Chemistry and Physics*. 56th ed. CRC Press Inc., 1975. Print. F-97, D141-146, B-1-2

Weisstein, Eric W. "Lead *Storage Battery -- from Eric Weisstein's World of Chemistry*." *ScienceWorld*. 1996-2007. Wolfram Research, Web. 7 Mar 2010. <http://scienceworld.wolfram.com/chemistry/LeadStorageBattery.html>.

Wenige, R., M. Niemann, U. Heider, M. Jungnitz, and V. Hilarius. "Liquid electrolyte Systems for Advanced Lithium Batteries." *Idustrial chemistry Symposium*. Seoul, Korea, Korean Institute of industrial Chemistry. 1997. 63-76. Print.

Woodbank Communications Ltd. "*Battery Management and Monitoring Systems BMS*." Electropaedia. 2005. Woodbank Communications Ltd, Web. 9 Mar 2010. <http://www.mpoweruk.com/bms.htm>.

Ye, M, Z-F Bai, and B-G Gao. "Energy recovery for battery electric vehicles." *Proceedings of the Institution of Mechanical Engineers, Part D: Journal of Automobile Engineering*. 222.10 (2008): 1827-1839. Print.

Zhao, Amy. "100AH LiFePO4 batteries." Message to Pierre Hinse. 28 Feb 2010. E-mail.

APPENDICES

```
Imports System
Imports System.IO
Imports PCComm

Public Class frmMain
    Private commGPS As New CommManager() : Private commDART As New CommManager() : Private transType _
        As String = String.Empty
    Dim LogFile As String = "Bus_DATA_" + DateTime.Now.ToString("yyyy-MM-dd-HH-mm") + ".csv"
    Dim sw As StreamWriter
    Dim LogMessage As String


    Private Sub Main_Load(ByVal sender As System.Object, ByVal e As System.EventArgs) Handles MyBase.Load
        LoadValues() : SetDefaults() : SetControlState()
    End Sub
    Private Sub LoadValues()
        commGPS.SetPortNameValues(cboPortGPS) : commGPS.SetParityValues(cboParityGPS) : _
          commGPS.SetStopBitValues(cboStopGPS)
        commDART.SetPortNameValues(cboPortDART) : commDART.SetParityValues(cboParityDART) : _
          commDART.SetStopBitValues(cboStopDART)
    End Sub
    Private Sub SetDefaults()


        cboPortGPS.SelectedIndex = cboPortGPS.FindStringExact("COM8") : cboBaudGPS.ResetText() : _
          cboBaudGPS.SelectedText = "38400"
        cboParityGPS.SelectedIndex = 0 : cboStopGPS.SelectedIndex = 1 : cboDataGPS.SelectedIndex = 1

        cboPortDART.SelectedIndex = cboPortDART.FindStringExact("COM1") : cboBaudDART.SelectedIndex = _
          cboBaudDART.FindStringExact("4800")
        cboParityDART.SelectedIndex = 0 : cboStopDART.SelectedIndex = 1 : cboDataDART.SelectedIndex = 1
        cboPortGPS.Enabled = True : cboBaudGPS.Enabled = True : cboParityGPS.Enabled = True
        cboStopGPS.Enabled = True : cboDataGPS.Enabled = True : btnStopLog.Enabled = False
        cboPortDART.Enabled = True : cboBaudDART.Enabled = True : cboParityDART.Enabled = True
        cboStopDART.Enabled = True : cboDataDART.Enabled = True : btnStartLog.Enabled = False
    End Sub
    Private Sub SetControlState()
        cmdSendGPS.Enabled = False : cmdSendDART.Enabled = False : cmdClose.Enabled = False : cmdOpen.Enabled = True
        cboPortGPS.Enabled = True : cboBaudGPS.Enabled = True : cboParityGPS.Enabled = True : cboStopGPS.Enabled = True
        cboDataGPS.Enabled = True : cboPortDART.Enabled = True : cboBaudDART.Enabled = True : _
          cboParityDART.Enabled = True
        cboStopDART.Enabled = True : cboDataDART.Enabled = True
    End Sub
    Private Sub GPS_BAUD(ByVal sender As System.Object, ByVal e As System.EventArgs)
        commGPS.BaudRate = cboBaudGPS.Text()
    End Sub
    Private Sub DART_BAUD(ByVal sender As System.Object, ByVal e As System.EventArgs)
        commDART.BaudRate = cboBaudDART.Text()
    End Sub
    Private Sub GPS_PARITY(ByVal sender As System.Object, ByVal e As System.EventArgs)
        commGPS.Parity = cboParityGPS.Text()
    End Sub
    Private Sub DART_PARITY(ByVal sender As System.Object, ByVal e As System.EventArgs)
        commDART.Parity = cboParityDART.Text()
    End Sub
    Private Sub GPS_STOPBITS(ByVal sender As System.Object, ByVal e As System.EventArgs)
        commGPS.StopBits = cboStopGPS.Text()
    End Sub
    Private Sub DART_STOPBITS(ByVal sender As System.Object, ByVal e As System.EventArgs)
        commDART.StopBits = cboStopDART.Text()
    End Sub
    Private Sub GPS_DATABITS(ByVal sender As System.Object, ByVal e As System.EventArgs)
        commGPS.DataBits = cboDataGPS.Text()
    End Sub
    Private Sub DART_DATABITS(ByVal sender As System.Object, ByVal e As System.EventArgs)
        commDART.DataBits = cboDataDART.Text()
    End Sub
    Private Sub cmdEXIT_Click(ByVal sender As System.Object, ByVal e As System.EventArgs)
        commDART.ClosePort() : commGPS.ClosePort() : End
    End Sub
    Private Sub cmdOpen_Click(ByVal sender As System.Object, ByVal e As System.EventArgs)
        cmdOpen.Enabled = False : cmdClose.Enabled = True : cboPortGPS.Enabled = False
        cboBaudGPS.Enabled = False : cboParityGPS.Enabled = False : cboStopGPS.Enabled = False
        cboDataGPS.Enabled = False : cboPortDART.Enabled = False : cboBaudDART.Enabled = False
        cboParityDART.Enabled = False : cboStopDART.Enabled = False : cboDataDART.Enabled = False
        commGPS.PortName = cboPortGPS.Text()
        commGPS.Parity = cboParityGPS.Text : commGPS.StopBits = cboStopGPS.Text : commGPS.DataBits = cboDataGPS.Text
        commGPS.BaudRate = cboBaudGPS.Text : commGPS.DisplayWindow = rtbDisplayGPS
        rbtGPSOpen.Checked = commGPS.OpenPort()
        commDART.PortName = cboPortDART.Text()
        commDART.Parity = cboParityDART.Text : commDART.StopBits = cboStopDART.Text : _
          commDART.DataBits = cboDataDART.Text
        commDART.BaudRate = cboBaudDART.Text : commDART.DisplayWindow = rtbDisplayDART
        rbtDARTOpen.Checked = commDART.OpenPort()
        cmdSendGPS.Enabled = True : cmdSendDART.Enabled = True : btnStartLog.Enabled = True
    End Sub
```

```
    Private Sub btnStartLog_Click(ByVal sender As System.Object, ByVal e As System.EventArgs)
        LogTimer.Enabled = True : btnStartLog.Enabled = False : btnStopLog.Enabled = True : btnClearData.Enabled =
False

    End Sub
    Private Sub btnStopLog_Click(ByVal sender As System.Object, ByVal e As System.EventArgs)
        LogTimer.Enabled = False : btnStartLog.Enabled = True : btnStopLog.Enabled = False : btnClearData.Enabled =
True

    End Sub
    Private Sub btnClearData_Click(ByVal sender As System.Object, ByVal e As System.EventArgs)
        If File.Exists(LogFile) Then File.Delete(LogFile)
        LogMessage = String.Empty
    End Sub
    Private Sub cmdSendGPS_Click(ByVal sender As System.Object, ByVal e As System.EventArgs)
        commGPS.Message = txtSendGPS.Text : commGPS.Type = CommManager.MessageType.Normal : _
          commGPS.WriteData(txtSendGPS.Text)
        txtSendGPS.Text = String.Empty : txtSendGPS.Focus()

    End Sub
    Private Sub cmdSendDART_Click(ByVal sender As System.Object, ByVal e As System.EventArgs)
        commDART.Message = txtSendDART.Text : commDART.Type = CommManager.MessageType.Normal : _
          commDART.WriteData(txtSendDART.Text)
        txtSendDART.Text = String.Empty : txtSendDART.Focus()

    End Sub
    Private Sub tmrUpdate_Tick(ByVal sender As System.Object, ByVal e As System.EventArgs) Handles tmrUpdate.Tick
        Dim wc As New Net.WebClient
        Dim longitude As String = String.Empty
        Dim latitude As String = String.Empty
        Dim zoom As String = "9"
        Dim key As String = "ABQIAAAA-saEOcQ4SYKZrqjKPfASPxSr66wH1vBfN5YhZjjpOB8XSIPqURR5YF7dftb7UnPMaBM7OhZmJv9cOA"
        Dim url As String = ""
        Dim width As String = ""
        Dim height As String = ""
        width = Convert.ToString(PictMAP.Width - 0)
        height = Convert.ToString(PictMAP.Height - 0)

        If CommManager.Longitude.Length > 9 And CommManager.Latitude.Length > 9 Then
            If CommManager.Longitude.Substring(9, 1) = "W" Then longitude = "-" + CommManager.Longitude.Substring(0,
8) _
                        Else longitude = CommManager.Longitude.Substring(0, 8)
            If CommManager.Latitude.Substring(9, 1) = "S" Then latitude = "-" + CommManager.Latitude.Substring(0, 8) _
                Else latitude = CommManager.Latitude.Substring(0, 8)

            url = "http://maps.google.com/staticmap?center=" + latitude + "," + longitude + "&zoom=17" + "&size=" + _
                width + "x" + height + "&maptype=hybrid" + "&key=" + key + "&sensor=true&format=jpg&frame=true"
            Try
                PictMAP.Image.Dispose()
            Catch ex As Exception
            End Try
            wc.DownloadFile(url, "map.jpg")
            PictMAP.Image = System.Drawing.Image.FromFile("map.jpg")
        End If
    End Sub
    Private Sub btnMapping_Click(ByVal sender As System.Object, ByVal e As System.EventArgs)
        If tmrUpdate.Enabled = True Then tmrUpdate.Enabled = False Else tmrUpdate.Enabled = True
    End Sub
    Private Sub LogTimer_Tick(ByVal sender As System.Object, ByVal e As System.EventArgs) Handles LogTimer.Tick +
        LogMessage = LogMessage + DateTime.Now.ToString(" MM/dd/yyyy HH:mm:ss.ff") + "," + CommManager.Axle_Count + _
           "," + CommManager.Distance + "," + _
        CommManager.Voltage + "," + CommManager.Speed_DART + "," + CommManager.kiloWatt + "," + CommManager.Amperage _
        + "," + CommManager.Latitude + "," + CommManager.Longitude + "," + CommManager.Altitude + "," + _
        CommManager.Speed_GPS + "," + CommManager.Course + vbCrLf

    End Sub
    Private Sub frmMain_Resize(ByVal sender As Object, ByVal e As System.EventArgs) Handles Me.Resize
        TabControl.Height = Me.Height - 11
        TabControl.Width = Me.Width - 37

    End Sub
    Private Sub cmdOpen_Click_1(ByVal sender As System.Object, ByVal e As System.EventArgs) Handles cmdOpen.Click
        cmdOpen.Enabled = False : cmdClose.Enabled = True : cboPortGPS.Enabled = False
        cboBaudGPS.Enabled = False : cboParityGPS.Enabled = False : cboStopGPS.Enabled = False
        cboDataGPS.Enabled = False : cboPortDART.Enabled = False : cboBaudDART.Enabled = False
        cboParityDART.Enabled = False : cboStopDART.Enabled = False : cboDataDART.Enabled = False
        commGPS.PortName = cboPortGPS.Text()
        commGPS.Parity = cboParityGPS.Text : commGPS.StopBits = cboStopGPS.Text : commGPS.DataBits = cboDataGPS.Text
        commGPS.BaudRate = cboBaudGPS.Text : commGPS.DisplayWindow = rtbDisplayGPS
        rbtGPSOpen.Checked = commGPS.OpenPort()
        commDART.PortName = cboPortDART.Text()
        commDART.Parity = cboParityDART.Text : commDART.StopBits = cboStopDART.Text : commDART.DataBits = _
          cboDataDART.Text
        commDART.BaudRate = cboBaudDART.Text : commDART.DisplayWindow = rtbDisplayDART
        rbtDARTOpen.Checked = commDART.OpenPort()
        cmdSendGPS.Enabled = True : cmdSendDART.Enabled = True : btnStartLog.Enabled = True
    End Sub
    Private Sub btnStartLog_Click_1(ByVal sender As System.Object, ByVal e As System.EventArgs) Handles
```

```
btnStartLog.Click
        LogTimer.Enabled = True : btnStartLog.Enabled = False : btnStopLog.Enabled = True : btnClearData.Enabled =
False
    End Sub
    Private Sub cmdClose_Click_1(ByVal sender As System.Object, ByVal e As System.EventArgs) Handles cmdClose.Click
        commDART.ClosePort() : commGPS.ClosePort() : SetControlState()
        rbtGPSOpen.Checked = False
        rbtDARTOpen.Checked = False
    End Sub
    Private Sub btnStopLog_Click_1(ByVal sender As System.Object, ByVal e As System.EventArgs) Handles _
          btnStopLog.Click
        LogTimer.Enabled = False : btnStartLog.Enabled = True : btnStopLog.Enabled = False : btnClearData.Enabled _
          = True
        If LogMessage <> String.Empty Then
            If Not File.Exists(LogFile) Then
                sw = File.CreateText(LogFile)
                sw.WriteLine(" Date/Time, Axle Count, Distance, Voltage, Speed, kiloWatt,
Amperage,Latitude,,Longitude,,Alt.,Speed,Course")
                sw.WriteLine(" MM/dd/yyyy HH:mm:ss.ff, xxxxx, Miles, Volts, mph, kW, Amps, deg, , deg, ,
meters,kph,deg")
                sw.Flush() : sw.Close()
            End If
            sw = File.AppendText(LogFile) : sw.WriteLine(LogMessage) : sw.Flush() : sw.Close()
            LogMessage = String.Empty
        End If

    End Sub
    Private Sub btnClearData_Click_1(ByVal sender As System.Object, ByVal e As System.EventArgs) Handles _
          btnClearData.Click
        If File.Exists(LogFile) Then File.Delete(LogFile)
    End Sub
    Private Sub cmdEXIT_Click_1(ByVal sender As System.Object, ByVal e As System.EventArgs) Handles cmdEXIT.Click
        commDART.ClosePort() : commGPS.ClosePort() : End
    End Sub
    Private Sub cmdSendGPS_Click_1(ByVal sender As System.Object, ByVal e As System.EventArgs) Handles _
          cmdSendGPS.Click
        commGPS.Message = txtSendGPS.Text : commGPS.Type = CommManager.MessageType.Normal : _
          commGPS.WriteData(txtSendGPS.Text)
        txtSendGPS.Text = String.Empty : txtSendGPS.Focus()

    End Sub
    Private Sub cmdSendDART_Click_1(ByVal sender As System.Object, ByVal e As System.EventArgs) Handles _
          cmdSendDART.Click
        commDART.Message = txtSendDART.Text : commDART.Type = CommManager.MessageType.Normal : _
          commDART.WriteData(txtSendDART.Text)
        txtSendDART.Text = String.Empty : txtSendDART.Focus()
    End Sub
    Private Sub btnExit_Click(ByVal sender As System.Object, ByVal e As System.EventArgs) Handles btnExit.Click
        commDART.ClosePort() : commGPS.ClosePort()
        If LogMessage <> String.Empty Then
            If Not File.Exists(LogFile) Then
                sw = File.CreateText(LogFile)
                sw.WriteLine(" Date/Time, Axle Count, Distance, Voltage, Speed, kiloWatt,
Amperage,Latitude,,Longitude,,Alt.,Speed,Course")
                sw.WriteLine(" MM/dd/yyyy HH:mm:ss.ff, xxxxx, Miles, Volts, mph, kW, Amps, deg, , deg, ,
meters,kph,deg")
                sw.Flush() : sw.Close()
            End If
            sw = File.AppendText(LogFile) : sw.WriteLine(LogMessage) : sw.Flush() : sw.Close()
            LogMessage = String.Empty
        End If
        End
    End Sub
    Private Sub btnGPSMAP_Click(ByVal sender As System.Object, ByVal e As System.EventArgs) Handles btnGPSMAP.Click
        If tmrUpdate.Enabled = True Then tmrUpdate.Enabled = False Else tmrUpdate.Enabled = True
    End Sub
    Private Sub TabControl_MouseClick(ByVal sender As Object, ByVal e As System.Windows.Forms.MouseEventArgs) _
          Handles TabControl.MouseClick
        If TabControl.SelectedTab.Text = "Immediate" And rbtGPSOpen.Checked Then
            If Not tmrRefresh.Enabled Then tmrRefresh.Enabled = True
        Else
            'tmrRefresh.Enabled = False
            'cboPortGPS.SelectedText = "COM8" : cboBaudGPS.SelectedText = "38400"
            'cboParityGPS.SelectedIndex = 0 : cboStopGPS.SelectedIndex = 1 : cboDataGPS.SelectedIndex = 1

            'cboPortDART.SelectedText = "COM1" : cboBaudDART.SelectedText = "4800"
            'cboParityDART.SelectedIndex = 0 : cboStopDART.SelectedIndex = 1 : cboDataDART.SelectedIndex = 1
        End If
    End Sub
    Private Sub tmrRefresh_Tick(ByVal sender As System.Object, ByVal e As System.EventArgs) Handles tmrRefresh.Tick
        'If CommManager.Voltage <> vbNull Then ngVolts.Value = Convert.ToSingle(CommManager.Voltage)
        'If CommManager.Amperage <> vbNull Then ngAmps.Value = Convert.ToSingle(CommManager.Amperage)
        'If CommManager.kiloWatt <> vbNull Then ngPower.Value = Convert.ToSingle(CommManager.kiloWatt)
        'If CommManager.Speed_DART <> vbNull Then ngSpeed.Value = Convert.ToSingle(CommManager.Speed_DART)
        tbImpDistance.Text = CommManager.Distance
        tbMetricDistance.Text = Convert.ToString(Convert.ToSingle(CommManager.Distance) * 1.609344)
        tbLongitude.Text = CommManager.Longitude
        tbLatitude.Text = CommManager.Latitude
    End Sub
End Class
```

Code Listing 1, Main Form Class.

```
Imports System
Imports System.IO
Imports System.Text
Imports System.Drawing
Imports System.IO.Ports
Imports System.Windows.Forms
Public Class CommManager
    Public Declare Function Inp Lib "inpout32.dll" Alias "Inp32" (ByVal PortAddress As Integer) As Integer
    Public Declare Sub Out Lib "inpout32.dll" Alias "Out32" (ByVal PortAddress As Integer, ByVal Value As Integer)
    Dim headerpos, endofstring As Integer
    ' public variables for display
    Public Shared Latitude As String = String.Empty
    Public Shared Longitude As String = String.Empty
    Public Shared Altitude As String = String.Empty
    Public Shared Speed_GPS As String = String.Empty
    Public Shared Course As String = String.Empty
    Public Shared Axle_Count As String = String.Empty
    Public Shared Distance As String = String.Empty
    Public Shared Voltage As String = String.Empty
    Public Shared Speed_DART As String = String.Empty
    Public Shared kiloWatt As String = String.Empty
    Public Shared Amperage As String = String.Empty
    Dim DARTMessage As String

#Region "Manager Enums"
    Public Enum MessageType
        Incoming
        Outgoing
        Normal
        Warning
        [Error]
    End Enum
#End Region
#Region "Manager Variables"
    Private _baudRate As String = String.Empty
    Private _LCR As Integer = 0
    Private _Port As Integer = 0
    Private _parity As String = String.Empty
    Private _stopBits As String = String.Empty
    Private _dataBits As String = String.Empty
    Private _portName As String = String.Empty
    Private _displayWindow As RichTextBox
    Private _msg As String
    Private _type As MessageType
    Private MessageColor As Color() = {Color.Blue, Color.Green, Color.Black, Color.Orange, Color.Red}
    Private comPort As New SerialPort()
    Private write As Boolean = True
#End Region
#Region "Manager Properties"
    Public Property BaudRate() As String
        Get
            Return _baudRate
        End Get
        Set(ByVal value As String)
            _baudRate = value
        End Set
    End Property
    Public Property Parity() As String
        Get
            Return _parity
        End Get
        Set(ByVal value As String)
            _parity = value
        End Set
    End Property
    Public Property StopBits() As String
        Get
            Return _stopBits
        End Get
        Set(ByVal value As String)
            _stopBits = value
        End Set
    End Property
    Public Property DataBits() As String
        Get
            Return _dataBits
        End Get
        Set(ByVal value As String)
            _dataBits = value
        End Set
    End Property
```

```
    Public Property PortName() As String
        Get
            Return _portName
        End Get
        Set(ByVal value As String)
            _portName = value
        End Set
    End Property
    Public Property DisplayWindow() As RichTextBox
        Get
            Return _displayWindow
        End Get
        Set(ByVal value As RichTextBox)
            _displayWindow = value
        End Set
    End Property
    Public Property Message() As String
        Get
            Return _msg
        End Get
        Set(ByVal value As String)
            _msg = value
        End Set
    End Property
    Public Property Type() As MessageType
        Get
            Return _type
        End Get
        Set(ByVal value As MessageType)
            _type = value
        End Set
    End Property
#End Region
#Region "Manager Constructors"
    Public Sub New(ByVal baud As String, ByVal par As String, ByVal sBits As String, ByVal dBits As String, ByVal name
As String, ByVal rtb As RichTextBox)
        _baudRate = baud : _parity = par : _stopBits = sBits : _dataBits = dBits : _portName = name : _
          _displayWindow = rtb
        AddHandler comPort.DataReceived, AddressOf comPort_DataReceived
    End Sub
    Public Sub New()
        _baudRate = String.Empty : _parity = String.Empty : _stopBits = String.Empty : _dataBits = String.Empty : _
          _portName = "COM1"
        _displayWindow = Nothing
        AddHandler comPort.DataReceived, AddressOf comPort_DataReceived
    End Sub
#End Region
#Region "WriteData"
    Public Sub WriteData(ByVal msg As String)
        If Not (comPort.IsOpen = True) Then comPort.Open()
        comPort.Write(msg) : _type = MessageType.Outgoing
        _msg = msg + "" + Environment.NewLine + "" : DisplayData(_type, _msg)
    End Sub
#End Region
#Region "DisplayData"
    <STAThread()> _
    Private Sub DisplayData(ByVal type As MessageType, ByVal msg As String)
        _displayWindow.Invoke(New EventHandler(AddressOf DoDisplay))
    End Sub
#End Region
#Region "OpenPort"
    Public Function OpenPort() As Boolean
        Try
            If comPort.IsOpen = True Then comPort.Close()
            comPort.BaudRate = Integer.Parse(_baudRate)
            comPort.DataBits = Integer.Parse(_dataBits)
            comPort.StopBits = DirectCast([Enum].Parse(GetType(StopBits), _stopBits), StopBits)
            comPort.Parity = DirectCast([Enum].Parse(GetType(Parity), _parity), Parity)
            comPort.PortName = _portName
            comPort.Open()
            Select Case _portName : Case "COM1" : _Port = &H3F8 : Case "COM2" : _Port = &H2F8
                Case "COM3" : _Port = &H3E8 : Case "COM4" : _Port = &H2E8 : End Select
            If Integer.Parse(_baudRate) < "8545" And Integer.Parse(_baudRate) > "7954" Then
                _LCR = Inp(_Port + 3) : Out((_Port + 3), (_LCR Or &H80)) : Out(_Port, 14)
                Out((_Port + 1), 0) : Out((_Port + 3), _LCR)
            End If
            Type = MessageType.Normal
            _msg = "Port opened at " + DateTime.Now + "" + Environment.NewLine + ""
            DisplayData(_type, _msg)
            Return True
        Catch ex As Exception
            DisplayData(MessageType.[Error], ex.Message)
            Return False
        End Try
    End Function
#End Region
```

```
#Region "ClosePort "
    Public Sub ClosePort()
        If comPort.IsOpen Then
            _msg = "Port closed at " + DateTime.Now + "" + Environment.NewLine + ""
            _type = MessageType.Normal
            DisplayData(_type, _msg)
            Try : comPort.Close() : Catch ex As Exception : End Try
        End If
    End Sub
#End Region
#Region "SetParityValues"
    Public Sub SetParityValues(ByVal obj As Object)
        For Each str As String In [Enum].GetNames(GetType(Parity))
            DirectCast(obj, ComboBox).Items.Add(str)
        Next
    End Sub
#End Region
#Region "SetStopBitValues"
    Public Sub SetStopBitValues(ByVal obj As Object)
        For Each str As String In [Enum].GetNames(GetType(StopBits))
            DirectCast(obj, ComboBox).Items.Add(str)
        Next
    End Sub
#End Region
#Region "SetPortNameValues"
    Public Sub SetPortNameValues(ByVal obj As Object)
        For Each str As String In SerialPort.GetPortNames()
            DirectCast(obj, ComboBox).Items.Add(str)
        Next
    End Sub
#End Region
#Region "comPort_DataReceived"
    Private Sub comPort_DataReceived(ByVal sender As Object, ByVal e As SerialDataReceivedEventArgs)
        Dim msg As String = comPort.ReadExisting()
        _type = MessageType.Incoming
        _msg = msg
        DisplayData(MessageType.Incoming, msg + "" + Environment.NewLine + "")
    End Sub
#End Region
#Region "DoDisplay"
    Private Sub DoDisplay(ByVal sender As Object, ByVal e As EventArgs)
        If sender.name = "rtbDisplayGPS" Then GPS_Data_Parser(sender, e)
        If sender.name = "rtbDisplayDART" Then DART_Data_Parser(sender, e)
        _displayWindow.SelectedText = String.Empty
        _displayWindow.SelectionFont = New Font(_displayWindow.SelectionFont, FontStyle.Bold)
        _displayWindow.SelectionColor = MessageColor(CType(_type, Integer))
        If _msg <> String.Empty Then _displayWindow.AppendText(_msg)
        _displayWindow.ScrollToCaret()
    End Sub
#End Region
#Region "Parse GPS DATA"
    Private Sub GPS_Data_Parser(ByVal sender As Object, ByVal e As EventArgs)
        If _msg <> String.Empty Then
            headerpos = _msg.IndexOf("$GPRMC")
            If headerpos > -1 Then
                If headerpos < (_msg.Length - 31) Then
                    Latitude = Convert.ToString(Convert.ToSingle(_msg.Substring(headerpos + 20, 2)) + _
                                                Convert.ToSingle(_msg.Substring(headerpos + 22, 7)) / 60) + "," + _
                                                _msg.Substring(headerpos + 30, 1)
                End If
                If headerpos < (_msg.Length - 44) Then
                    Longitude = Convert.ToString(Convert.ToSingle(_msg.Substring(headerpos + 32, 3)) + _
                                                 Convert.ToSingle(_msg.Substring(headerpos + 35, 7)) / 60) + "," + _
                                                 _msg.Substring(headerpos + 43, 1)
                End If
                If headerpos < (_msg.Length - 46) Then
                    endofstring = _msg.IndexOf(",", headerpos + 46)
                    If endofstring > -1 Then Speed_GPS = _msg.Substring(headerpos + 45, endofstring - headerpos - 45)
                End If
            End If
            headerpos = _msg.IndexOf("$GPVTG")
            If headerpos > -1 Then
                If headerpos < (_msg.Length - 13) Then Course = _msg.Substring(headerpos + 7, 6)
            End If
            headerpos = _msg.IndexOf("$GPGGA")
            If headerpos > -1 Then
                endofstring = _msg.IndexOf(",M,", headerpos)
                If endofstring > -1 Then Altitude = _msg.Substring(endofstring - 5, 5)
            End If
            If Latitude = String.Empty Then Latitude = ",,"
            If Longitude = String.Empty Then Longitude = ",,"
        End If
    End Sub
#End Region
```

```
#Region "Parse DART DATA"
    Private Sub DART_Data_Parser(ByVal sender As Object, ByVal e As EventArgs)
        If _msg <> String.Empty Then
            Dim pol As String
            DARTMessage = DARTMessage + _msg
            If DARTMessage.LastIndexOf(":") > 0 And (DARTMessage.Length) > (DARTMessage.LastIndexOf(":") + 27) Then
                DARTMessage = DARTMessage.Substring(DARTMessage.LastIndexOf(":"))
                If DARTMessage.Substring(23, 1).Equals("0") Then pol = "-" Else pol = "+"
                Axle_Count = DARTMessage.Substring(1, 8)
                Distance = Convert.ToString(Convert.ToSingle(DARTMessage.Substring(9, 4)) / 10)
                Voltage = DARTMessage.Substring(14, 3)
                Speed_DART = DARTMessage.Substring(17, 2)
                kiloWatt = Convert.ToString(Convert.ToSingle(pol + DARTMessage.Substring(19, 4)) / 10)
                Amperage = pol + DARTMessage.Substring(24, 3)
                DARTMessage = String.Empty
            End If
        End If
    End Sub
#End Region
End Class
```

Code Listing 2, CommManager Class.

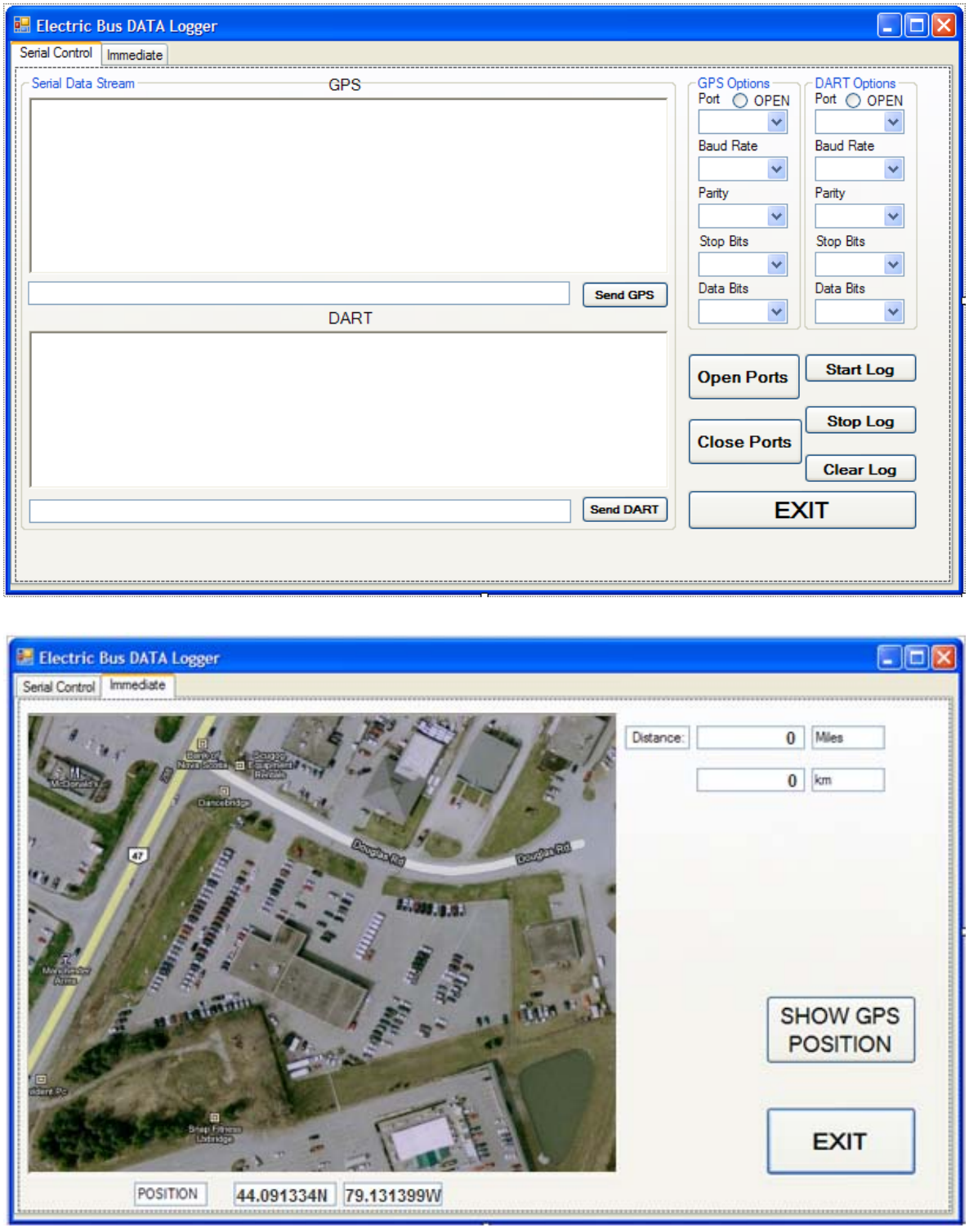

Figure 36, Data Collection Program Main GUI

```
Vehicle:
      Transmission = 'Single reduction'
      Axle = '2 wheel drive'
      Power = 'Electric'
      Driver Model = 'drv_prime_mover_electric_equation'
      Driver initialization = 'drv_bus_20000_50'

ESS:
      ESS Model = 'ess_generic_map'
      ESS Technology = 'nicd'
      ESS Initialization = 'ess_nicd_102_125'
      SOC Initialization = 100 %
      SOC Minimum = 40 %
      SOC Maximum = 100 %
      ESS Number of Cells in Series = 270
      ESS Cells in Parallel = 2
      ESS Packaging Factor = 1.25
      ESS Cell Capacity = 180 Ah
      ESS Cell Nominal Voltage = 2 Volt

Drivetrain:
      Motor Mass = 200 kg
      Controller Mass = 20 kg
      Minimum Voltage = 270 Volt
      Maximum current = 300 Amp
      Drivetrain mass = 50 kg
      Final Drive Mass = 400 kg
      Final Drive Ratio = 5.8

Axles:
      Number of Wheels = 4
      Mass per Wheel = 100 kg
      Inertia per Wheel = 0.5 kgm^2
      Wheel Theoretical Radius = 0.3935 m
      Wheel Radius Correction Factor = 0.95
      Wheel Initial Radius = 0.3738 m
      Wheel Rolling Friction Coefficient1 = 0.0011
      Wheel Rolling Friction Coefficient2 = 0.0001

Vehicle Body:
      Vehicle Initial Body Mass = 7570 kg
      Vehicle Cargo Mass = 0 kg
      Vehicle Frontal Area = 7 m^2
      Vehicle Drag Coefficient = 0.5
      Vehicle Front/Rear Ratio = 0.3
      Vehicle Initial Mass = 7570 kg
      (parameter override from measurement)

Accessories:
      DC/DC Inverter Mass = 18 kg
      Accessory load = 2 kW

Regenerative Braking:
```

```
Vehicle:
      Transmission = 'Automatic'
      Axle = '2 wheel drive'
      Power = 'Diesel CI'
      Driver Model = 'drv_conv_dm_equation'
      Driver initialization = 'drv_bus_20000_50'

Engine:
      Engine Model = 'eng_map_hot'
      Engine Technology = 'CI'
      Engine Initialization = 'eng_ci_6500_119'
      Engine Initialization Model= 'eng_s_lin_hot_and_cold'
      Engine Displacement = 6.5 L
      Engine Map = 'eng_hot'
      Engine Mass = 508 kg
      Engine Fuel Mass = 100 kg
      Engine Fuel Tank Mass = 30 kg

Drivetrain:
      Transmission Mass = 333 kg
      Transmission Inertia In = 0.003 kgm^2
      Transmission Inertia Out = 0 kgm^2
      Transmission Speed Threshold = 10 rad/s

Axles:
      Number of Wheels = 4
      Mass per Wheel = 100 kg
      Inertia per Wheel = 0.5 kgm^2
      Wheel Theoretical Radius = 0.3935 m
      Wheel Radius Correction Factor = 0.95
      Wheel Initial Radius = 0.3738 m
      Wheel Rolling Friction Coefficient1 = 0.0011
      Wheel Rolling Friction Coefficient2 = 0.0001

Vehicle Body:
      Vehicle Initial Body Mass = 6500 kg
      Vehicle Cargo Mass = 0 kg
      Vehicle Frontal Area = 7 m^2
      Vehicle Drag Coefficient = 0.79
      Vehicle Front/Rear Ratio = 0.4
      Vehicle Initial Mass = 6500 kg
      (parameter override to match electric bus)

Accessories:
      Electrical Accessory load = 1 kW
      Mechanical Accessory Load = 2kW
```